G-Safety
SCIENCE FOR GLOBAL SAFETY

2nd International Symposium on Water Environment Systems

---with Perspective of Global Safety

(January 30-31 , 2015)

Dept. of Civil and Environmental Engineering
Graduate School of Engineering
Tohoku University

TOHOKU
UNIVERSITY

Sponsors

http://www.g-safety.tohoku.ac.jp/
Tohoku University, Main Administration Office Organization for Leading Graduate School Program of Tohoku University, Sendai, Miyagi 980-8578, Japan

http://www.eng.tohoku.ac.jp/
Tohoku University, Graduate School of Engineering, Sendai, Miyagi 980-8579, Japan

ORGANIZERS

Dr. So Kazama (Professor, Tohoku University)

Dr. Osamu Nishimura (Professor, Tohoku University)

Dr. Yu-You LI (Professor, Tohoku University)

Dr. Daisuke Komori (Associate Professor, Tohoku University)

STUDENT SECRETARIES

DC Student, Yanlong ZHANG
E-mail: zhangyl@epl1.civil.tohoku.ac.jp

MC student, Toshiki SUGO
E-mail: sogo@epl1.civil.tohoku.ac.jp

MC student, Yizhe ZHENG
E-mail: Zhengyz@epl1.civil.tohoku.ac.jp

PARTICIPANTS

Tohoku university		**JAPAN**
Name	**Identity**	**E-mail**
Adriana	P.D.	adriana@epl1.civil.tohoku.ac.jp
Yanlong ZHANG	Student	Zhangyl@epl1.civil.tohoku.ac.jp
Xueqing LU	Student	luxq@epl1.civil.tohoku.ac.jp
Yuan LIU	Student	liuyuan@epl1.civil.tohoku.ac.jp
Toshiki SUGO	Student	sugo@epl1.civil.tohoku.ac.jp
Yu QIN	Student	qinyu@epl1.civil.tohoku.ac.jp
Haiyuan MA	Student	mahy@epl1.civil.tohoku.ac.jp
Yizhe ZHENG	Student	Zhengyz@epl1.civil.tohoku.ac.jp

Xi'an university of architecture and Technology		**CHINA**
Name	**Identity**	**E-mail**
Dangcong PENG	Professor	dcpeng@xauat.edu.cn
Yun HAN	Associate Professor	hanyun@xauat.edu.cn
Yongmei ZHANG	Student	zym58625@163.com
Jialing TANG	Student	921221788@qq.com

Southeast university		**CHINA**
Name	**Identity**	**E-mail**
Hailiang SONG	Associate Professor	songhailiang@seu.edu.cn
Feng HONG	Assistant Professor	hong4796@seu.edu.cn
Yuli YANG	Student	230149398@seu.edu.cn
Xizi LONG	Student	230149343@seu.edu.cn

PARTICIPANTS

Beijing Normal university		**CHINA**
Name	**Identity**	**E-mail**
Baolin SU	Professor	subl@bnu.edu.cn

Universiti Teknologi Malaysia		**MALAYSIA**
Name	**Identity**	**E-mail**
Fadhil	Associate Professor	mfadhil@utm.my
Nickholas Anting Anak Guntor	Student	nickholasanting@gmail.com

Sultan Qaboos University		**OMAN**
Name	**Identity**	**E-mail**
Luminda GUNAWARDHANA	Assistant Professor	luminda@squ.edu.om

Indian Institute of Technology Hyderabad		**INDIA**
Name	**Identity**	**E-mail**
Basudev Biswal	Assistant Professor	basudev@iith.ac.in

Access to Aobayama Campus
School of Engineering

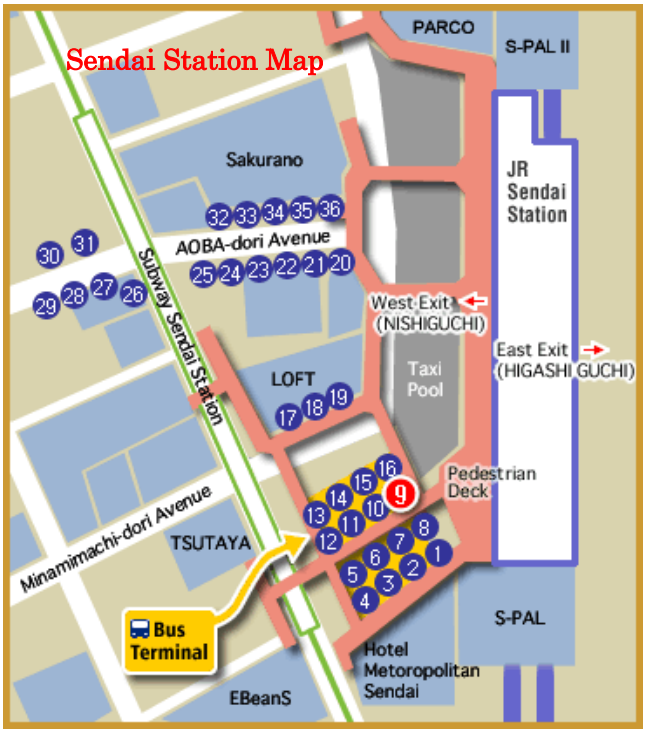

Buses leave the bus terminal at the JR Sendai Station (bus stop No. 9) every 30 minutes for the 20-minutes trip to the "**Kogakubu-chuo**" bus stop in front of the School of Engineering.

Buses Numbers
S710-715, 719, 750, or 757

Venue

Aobayama campus, Tohoku University
Meeting Room-A (105) of civil engineering and architecture. (Morning)
Complex building, Room 101. (Afternoon)

Aobayama Campus Map

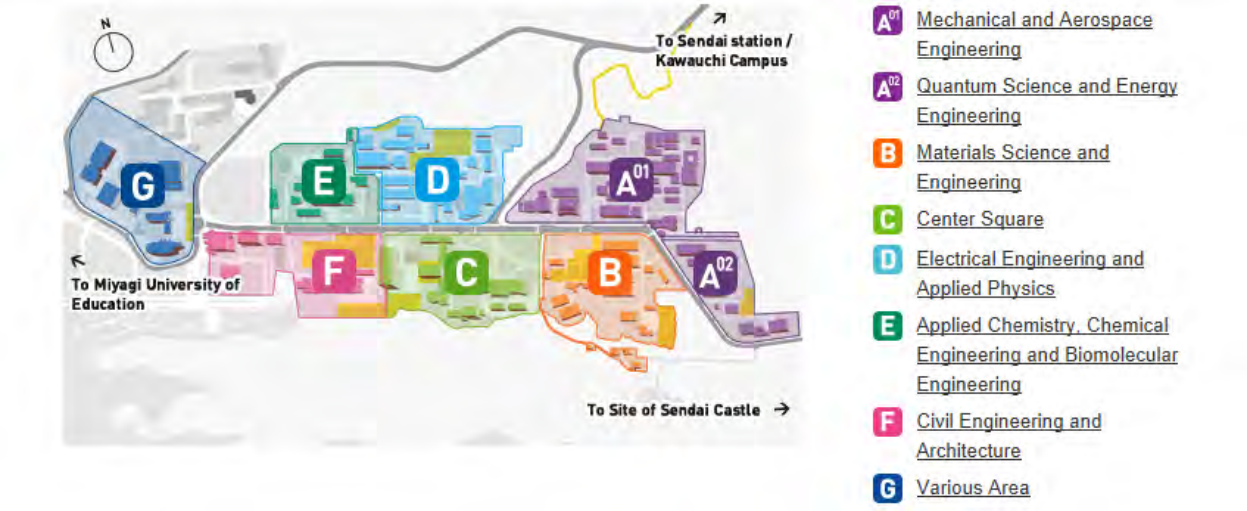

Meeting Room-A (Room105)

Complex building (Room101)

Program

January 30, 2015

10:00~11:00 | **Lab Visit**

Meeting at the Meeting Room-A (Room105) of civil engineering and architecture.

Place: Laboratory building of civil and environmental engineering.

11:00~12:00 | **Session I, Poster exhibition and free discussion**

Place: Meeting Room-A (Room105) of civil engineering and architecture.

	" Operation performance of upflow anaerobic sludge blanket (UASB) reactor treating starch wastewater " **Xueqing LU** (Tohoku University)
	"Reaction evolution to one-stage anammox in a partial nitritation reactor" **Yuan LIU** (Tohoku University)
	"Effect of Substrate Concentration on the Operation Performance of Anammox Process in a UASB Reactor " **Haiyuan MA**(Tohoku University)
	"Current state of knowledge of antibiotics in the environment: a global approach" **Adriana**(Tohoku University)
	"Phase Separation by Hyper-thermophilic Temperature in Anaerobic Digestion of Waste Activated Sludge" **Yu QIN** (Tohoku university, Japan)

12:00~13:00 | **Lunch**

Place: The main cafeteria in Aobayama Campus

13:00~13:10 | **Organizer Opening address** (Prof. Yu-You Li, Tohoku University)

Place: Complex building Room No.101

13:10~13:20 | **Memorial Photo**

Place: Complex building Room No.101

13:30~16:00 | Session II, Special lecture

13:30 – 14:00	"River Discharge Variations Attributed to Extreme Rainfall in Oman" **Dr. Luminda Gunawardhana** (Sultan Quboos University, Oman)
14:00 – 14:30	"A field-scale observation method for non-point source pollution of paddy fields" **Dr. Baolin SU** (Beijing Normal University, China)
14:30 – 15:00	"Algae as Energy Securing, Supplement Reserve and Formulating Carbon Sequestration for Waste Management from Palm Oil Mill Effluent (POME)" **Dr. Fadhil** (Universiti Teknologi Malaysia, Malaysia)
15:00-15:30	"Enhancement of Biogas Productivity through Bio-pretreatment of Crop residue during Anaerobic Digestion" **Dr. Feng HONG** (Dongnan University, China)
15:30-16:00	"Geomorphological recession flow model for estimation of drainable storage" **Dr. Basudev Biswal** (Indian Institute of Technology Hyderabad, India)

16:00~16:15 | Coffee break

16:15~18:15	Session III, Presentations by students

Place: Complex building Room No.101

16:15~16:30	"Preparation and evaluation of fermentation liquid of food waste as a carbon source for denitrification" **Yongmei ZHANG** (Xi'an university of architecture and Technology, China)
16:30~16:45	"Nitrogen removal enhancement in A/O-MBR with fermentation liquid of food waste (FLFW) as external carbon" **Jialing TANG** (Xi'an university of architecture and Technology, China)
16:45~17:00	"Structure Optimization of Constructed Wetland Coupled Microbial Fuel Cell for Organism Removal" **Xizi LONG** (Dongnan University, China)
17:00~17:15	"Analysis of enhanced nitrogen removal in MBR with new biological carriers addition by real-time PCR" **Yuli YANG** (Dongnan University, China)
17:15~17:30	"Effect of oysters on size-fractionated marine phytoplankton communities in Shizugawa bay" **Yizhe ZHENG** (Tohoku university, Japan)
17:30~17:45	"Evaluation of new sewage treatment system using anaerobic membrane bioreactor" **Sugo TOSHIKI** (Tohoku university, Japan)
17:45~18:00	"Study of the start-up and inhibition process of Anammox reaction in UASB Reactor" **Yanlong ZHANG** (Tohoku university, Japan)
18:00~18:15	"Innovation of cool-pavement technology from waste tile" **Nickholas Anting** (Universiti Teknologi Malaysia, Malaysia)

18:15~18:25	Closing speech

January 31, 2015 Fieldwork

Minami-Gamo Sewage Treatment Plant

Tsunami was hitting Sewage Facilities

Effect on the wall of pump station

Session I

Poster exhibition and free discussion

Operation performance of upflow anaerobic sludge blanket (UASB) reactor treating starch wastewater

○Xueqin Lu[1], Guangyin Zhen[2], Adriana Ledezma Estrada[1], Yu-You Li[1]*

[1]Department of Civil and Environmental Engineering,Tohoku University,Sendai,Miyagi 980-8579, Japan
[2]National Institute for Environmental Studies, Onogawa 16-2, Tsukuba, Ibaraki 305-0053, Japan
*E-mail: yyli@epl1.civil.tohoku.ac.jp

Abstract

Long-term performance of a lab-scale UASB reactor treating starch wastewater was investigated under different hydraulic retention times (HRT). Successful start-up could be achieved after 15 days' operation. The optimal HRT was 6 h with organic loading rate (OLR) 4 g COD/L•d at COD concentration 1000 mg/L, attaining 81.1–98.7% total COD removal with methane production rate of 0.33 L CH_4/g $COD_{removed}$. Specific methane activity tests demonstrated that methane formation via H_2-CO_2 and acetate were the principal degradation pathways. Vertical characterizations revealed that main reactions including starch hydrolysis, acidification and methanogenesis occurred at the lower part of reactor ("main reaction zone"); comparatively, at the up converting acetate into methane predominated ("substrate-shortage zone"). Further reducing HRT to 3 h caused volatile fatty acids accumulation, sludge floating and performance deterioration.

Keywords: UASB, starch wastewater, granule sludge, Specific methane activity

1. Introduction

Starch, composed of repeating *D*-glucopyranosyl units, are largely used in human and animal nutrition, or as virgin materials for a wide range of industrial products. The increased adopts of starch inevitably lead to the production of massive starch wastewater. One such type of wastewater, with COD 25 g/L and low pH 3.8–5.2, for instance, was harvested from about 250 existing small-scale plants by the starch extraction process which was discharged to water bodies without any treatment. The limited knowledge achieved until now yet cannot definitely answer whether UASB proceeds smoothly during the long-term operation if starch is added solely.

Therefore, in this study, a lab-scale UASB reactor has been constructed and operated for more than 200 days to comprehensively evaluate the long-term performance of UASB in treating starch wastewater. The effects of OLR on the overall stability were examined by varying HRT (from 24 to 3 h) to optimize the operating condition. Besides, the possible changes of water qualities (i.e. pH, ORP, COD, acetate, etc.) and granule characteristics along the height were detected, hoping to map the core degradation dynamics occurred in the interior of UASB.

2. Materials and Methods

The schematic diagram of the UASB reactor is depicted in (Fig. 1). The set-up designed herein consists of a starch wastewater feed tank, a temperature control unit, UASB main body, a wet gas flow meter and a desulfidation unit. The operational temperature was kept constant at 35 ± 1 ˚C using a heated water bath.

The synthetic wastewater was composed of (mg/L): 1000 CODstarch, 2000-2700 $NaHCO_3$, 850 NH_4Cl, 750 KCl, 250 K_2HPO_4, 100 KH_2PO_4, 125 $MgCl_2$•$6H_2O$, 4.2 $NiCl_2$•$6H_2O$, 4.2 $CoCl_2$•$6H_2O$, 15 $CaCl_2$•$2H_2O$ and 42 FeCl•$4H_2O$.

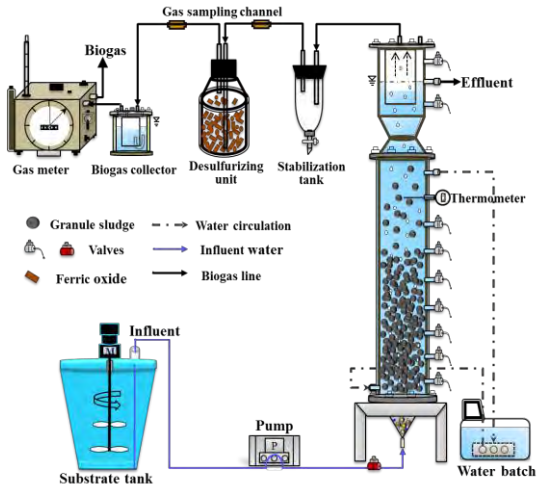

Fig. 1 Schematic diagram of the UASB reactor system.

3. Results and discussion

3.1 Roles of OLR on biogas production and COD removal

The results showed that the performance of UASB system strongly depended on OLR applied (Fig. 2). As presented in Fig. 2a, biogas production rate showed a closely positive correlation with OLR, and increased linearly with OLR ($R = 0.9846$, $p < 0.01$), agreeing well with the investigations of Parthiban et al. (2007) on anaerobic tapered fluidized bed reactor fed with starch wastewater. On the other hand, methane content in biogas reached a maximum, up to 78% at 4 g COD/L•d (i.e. HRT 6 h) and then dropped down with the further increasing of OLR. Meanwhile, with the OLR increasing from 1 to 8 g COD/L•d, TCOD and SCOD removal also declined to some extents, possibly owing to higher upflow velocity (V_{up}) which reduced the contact time between granules and targets present in wastewater in addition to smashing and resultantly higher washout of sludge granules.

Hence, taking into account efficient bioenergy recovery and continuous stability of the system, the optimum OLR in the present study should be 4 g COD/L•d, i.e. HRT 6 h. Furthermore, the relationship between OLR and UASB performance in stable and recovery stages were compared (i.e. at HRT of 24, 12 and 6 h), and the results are graphically reported in Fig. 2b. Biogas production and COD removal were less stable and efficient in recovery stage in comparison with the stable stage at the same OLR conditions. In this situation, biogas production gave a very poor correlation with OLR (R^2 = 0.5679), in sharp contrast with the perfect linear increment under stable operations (R^2

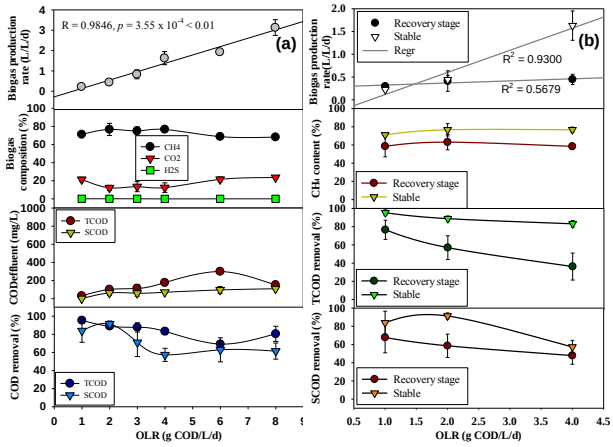

Fig. 2. Effect of OLR on UASB performance under normal and recovery phase.

3.2 Possible biodegradation mechanisms of starch in UASB

Specific methanogenic activity test was conducted to in-depth understand the decomposition mechanisms of starch. The tests with H_2-CO_2 and four volatile fatty acids (i.e. formate, acetate, propionate and butyrate) revealed that

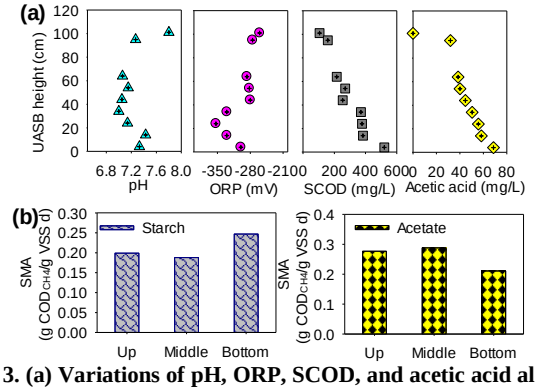

Fig. 3. (a) Variations of pH, ORP, SCOD, and acetic acid along the height of UASB; (b) SMA of granular sludges sampled from the up, middle and bottom.

Vertical characterizations (Fig. 3) indicated that main reactions including starch hydrolysis, acidification and methanogenesis occurred at the lower part of reactor ("main reaction zone"); while at the up converting acetate into methane predominated ("substrate-shortage zone"). Bottom-granules could efficiently utilize both starch and acetic acid for methane recovery, with SMA value of 0.247, and 0.211 g $CODCH_4$/g VSS•d, respectively; the granular sludges from the middle and up, in contrast, were capable of decomposing acetate (0.277–0.288 g $CODCH_4$/g VSS•d), but exhibited the poor decomposition capability to starch (0.188–0.199 g $CODCH_4$/g VSS•d). In this sense, the co-growth of starch- and acetate-utilizing microbes at the bottom were predominant while the unique microorganisms feeding on acetate grew in abundance at the up. The dynamic distribution of key populations in the reactor did not only increase the resistance of microbes against the external stress, but also improved the overall operating stability.

3.3 Characterization of granular sludge in the UASB

The granular sludges, after 104 days of operating, were collected from different positions of UASB by SEM analysis. The granules from the up and middle mainly comprised of rod-shaped archaebacterial (Fig. 4b-c); the cells closely associated with or entrapped within sludge matrix, forming a compact and intact micro-structure.For the granules from the bottom, not only rod-shaped archaebacterial also cocci-shaped archaea prevailed on the surface or interior of granules (Fig. 4d).

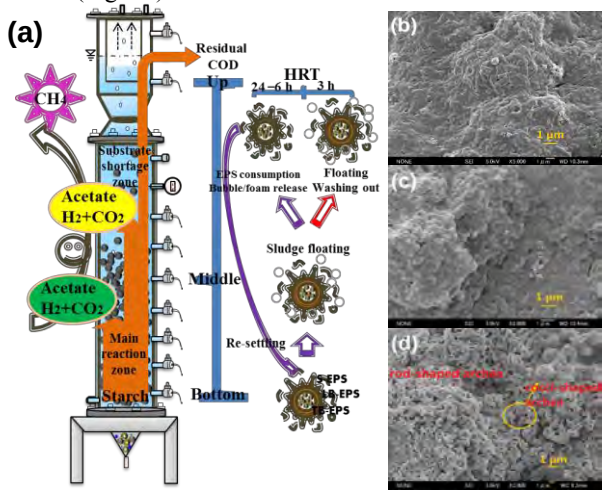

Fig. 4 Starch fermentation dynamics and principal mechanisms of sludge floating in the interior of UASB (a); SEM images of granules collected from (b) up; (c) middle; and (d) bottom.

Starch indicated by SCOD at the bottom was the highest (Fig. 3a); and it was gradually metabolized, attenuated along the upflow direction (i.e. from the bottom to up) and nearly diminished at the up. Likewise, acetic acid derived from starch exhibited a similar variation, peaking at the bottom and there was extremely low residual acetic acid detected at the up. From the experimental data, it can be speculated that the reactions taking place between the bottom and middle in UASB were the hydrolysis of starch, accompanied by the formation of acetate (i.e. acidification) and concurrent utilization (i.e. methanogenesis); therefore, the zone could be called the "main reaction zone". Comparatively, thanks to the efficient degradation of starch previously, converting acetate into methane (i.e. methanogenesis) at the up predominated (i.e. "substrate-shortage zone") (Fig. 4a).

4. Conclusions

(1) UASB showed good performance for treating starch wastewater. The optimal HRT was 6 h with OLR 4 g COD/L•d, gaining 81.1–98.7% COD removal and 0.33 L CH_4/g CODremoved methane yield.

(2) Methane production via H_2-CO_2 and acetate were the principal starch fermentation pathways, which occurred at the lower part of reactor while at the up converting acetate into methane predominated.

Reaction evolution to one-stage anammox in a partial nitritation reactor

○Yuan LIU[1], Jiayuan[1] JI, Toshimasa HOJO[2], Yu-You LI[1,2*]

[1]Graduate School of Environmental Studies, Tohoku University, Sendai 980-8579, Japan
[2]Graduate School of Engineering, Tohoku University, Sendai 980-8579, Japan
*E-mail: yyli@epl1.civil.tohoku.ac.jp

Abstract

This study investigated partial nitritation achievement and maintenance in a CSTR reactor. The reactor was operated at temperature range of 25~33℃ and pH between 8.0-8.5. Under the comprehensive effect of DO limitation, nitrite accumulation and partial nitritation was achieved successfully. The effect of variation of DO concentration in the reactor on the efficiency of NH_4^+-N conversion to NO_2^--N and ratio of NO_2^--N/NH_4^+-N in the effluent was evaluated. Results showed that when DO concentration was kept as 0.13mg/L or AR was set as 1.60L/min, the optimum NO_2^--N/NH_4^+-N ratio can be achieved and long-term maintained. Subsequently, by adjusting AR, the one-stage anammox was achieved and the maximum nitrogen removal rate was gained when AR was kept as 1.50L/min.

Keywords: partial nitritation, one-stage anammox, low C/N, biological nitrogen removal

1. Introduction

Anammox, the most innovative process discovered in the early 1990s, converts NH_4^+ and NO_2^- to N_2 with the absence of oxygen and organic carbon sources has arisen great expectations regarding elimination of N high-loaded wastewaters containing low biodegradable organic carbon to nitrogen (C/N) ratio. In brief, anammox process consists of (1) partial nitritation (PN) in which 57% of NH_4^+ was oxidized in to NO_2^- and (2) anammox (A) by which the additional NH_4^+ and produced NO_2^- in (1) process were removed as N_2 and a small amount of nitrate. Two different strategies are used for anammox establishing: NO_2^- can be either produced in a separate aerated reactor and subsequently be fed into an anoxic anammox reactor named as two-stage PN/A or accumulated in the same reactor with anammox process that is one-stage PN/A.

Over the last decade, the cumulative nitrogen load increased almost 60-fold, indicating that from an economic perspective, the anammox-based processes are becoming increasingly widespread. Recently many technologies have been developed and studied for their applicability to the PN/A concept and several have made it into full-scale. It was predicted that by 2014 100 full-scale installations will be in operation worldwide. More than 50% of all PN/A installations in application are sequencing batch reactors, 88% of all plants being operated as single-stage systems, and 75% for side-stream treatment of municipal wastewater.

With respect to two-stage PN-anammox process, there are two requirements needed to be met in this system: (1) the nitrite accumulation rate ($\eta=NO_2^-N/NO_x^-N\times 100\%$, where $NO_x^-N=NO_2^-N+NO_3^-N$) should be high since nitrate is not the direct substrate of anammox; (2) nitrite and ammonium should be at an approximate equimlar ratio (NH_4^+N/NO_2^-N = 1:1.32). And it is a significant research issue that exploring a practical operation for long-term of 50~60%% of partial nitritation maintenance. When it comes to one-stage process, both groups of bacteria need to be in the right redox environment, which can be achieved by carefully controlling the bulk oxygen concentration.

The goal of this research were to (i) establish a robust method to rapidly partial nitritation achievement and long-term maintenance; (ii) autotrophic N removal from NH_4^+ in an aerated lab-scale reactor.

2. Materials and Methods

2.1 Experiment configuration and operation conditions

As shown in Fig.1, the partial nitritation was carried out in a lab-scale continuous stirred-tank reactor (CSTR), which is made of a transparent PVC plastic rectangular reactor with working volume of 8 liters and settling zone volume of 2L.The temperature in the reactor were set and keep in the range of 25~33℃ by a heater with temperature adjuster set in the reaction zone. Dissolved oxygen (DO) concentration was controlled in low concentration, and adjusted to a series of concentrations in order to obtain the optimum results. The hydraulic retention time (HRT) was kept as 12 h, nitrogen

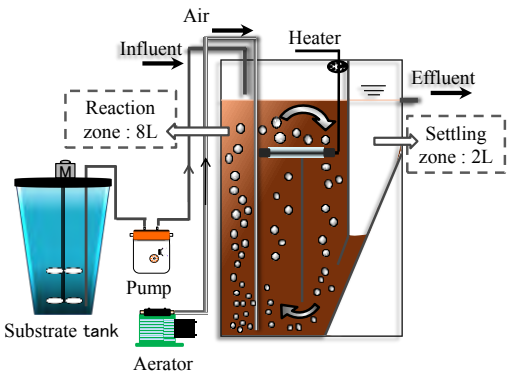

Fig. 1 Schematic diagram of partial nitritation reactor

loading rate in the operation period was 0.5kgNH_4^+-N/m^3/d.

2.2 Synthetic wastewater and seed sludge

During the whole operation period, the reaction was feeding with synthetic wastewater and trace element shown in Table 1, in which the NH_4^+-N concentration was 250 mg/L. pH in the substrate was adjusted in a range of 8.0~8.5 by adding of buffer agents consist of $NaHCO_3$, KH_2PO_4 and K_2HPO_4. The seed sludge was obtained from S Municipal wastewater treatment plant and was cultivated by full-and-draw technique before transferring it into the reactor. The initial mixed liquor suspended solid (MLSS) concentration of the reactor was set at 2000 mg/L.

2.3 Methodology

The MLSS were determined according to the Standard Methods (APHA, 2002). Ammonium, nitrite and nitrate concentrations were detected by capillary electrophoresis of Agilent 7100 (M. Vilas-Cruz, 1994). DO concentration and pH were measured by a portable DO and pH meter.

3. Results and Discussion

3.1. Establish of long-term partial nitritation

The exploration of method to long-term partial nitritaion was conducted during Phase I. The changes of DO concentration, AR, nitrogen concentrations in the reactor during the operation period are shown in Fig.2. As Do concentration was controlled as lower than 0.8mg/L since the first day, which was favor to ammonia oxidizing bacteria (AOB) compare to nitrite oxidizing bacteria (NOB), majority of ammonia was oxidized into NO_2^--N. When DO concentration was further decreased gradually, the AOB activity was restricted and the ratio of NO_2^--N/NH_4^+-N (as shown in Fig.3) also decreased correspondingly. By adjusting the DO concentration and aeration rate (AR) in the reactor, the relationship between DO, AR and NO_2^--N/NH_4^+-N ratio showed that when DO concentration was kept as 0.13mg/L or AR was set as 1.60L/min, the optimum NO_2^--N/NH_4^+-N ratio can be achieved and long-term maintained, which met the requirement of anammox reaction.

3.2. Reaction evolution to one-stage anammox

As shown in Fig.2, during day 242~day 264 in Phase I, a slight amount of nitrogen removal was achieved with the nitrogen removal rate (NRR) as about 13%. However, as shown in Fig.3 the ratio of NO_3^--N/NH_4^+-N showed that the nitrate production during this period was a little lower than theoretical value by anammox reaction. In order to promote anammox reaction rate, AR was gradually decreased in Phase II (day 265~day310), with the result that NRR increased to 25% while a great mount of ammonia was still remained in the reactor. Subsequently, as a result of AR was increased into 1.50L/min, nitrogen removal was correspondingly enhanced up. During this period, the concentration of NH_4^+-N decreased slowly and it came through about 50 days before the NRR achieved the maximum 88.8%. In addition, the ratio of NO_3^--N/NH_4^+-N in Fig.3 showed that the nitrate production during this period was at the same level to theoretical value by anammox reaction, which can be deduced that nitrogen

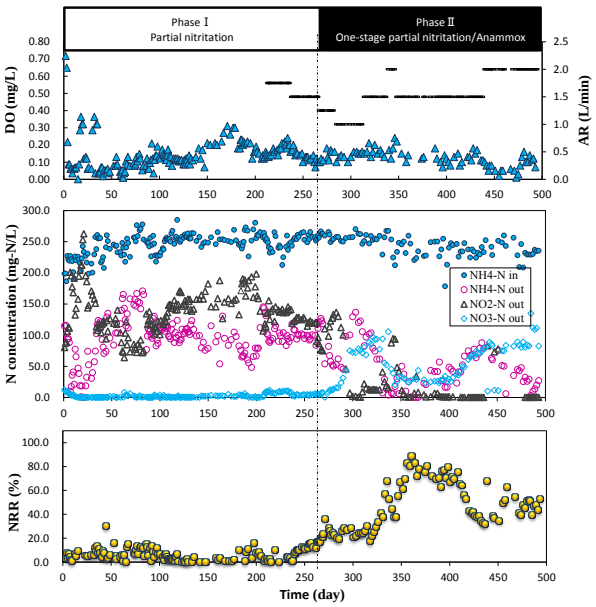

Fig. 2 Changes of DO concentration, AR, nitrogen concentrations and NRR in the reactor

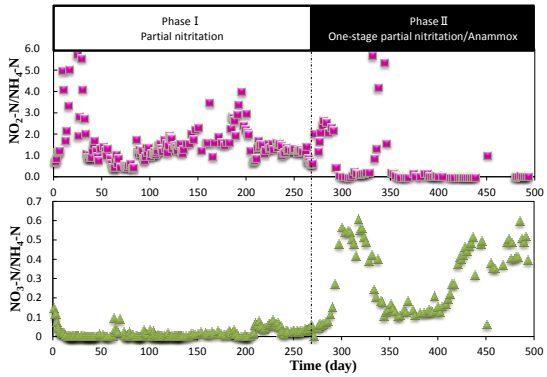

Fig. 3 Variations of NO_2^--N/NH_4^+-N and NO_3^--N/NH_4^+-N during the operation period

removal during this period was caused by typical one-stage anammox process. The higher nitrogen removal (over 65%) was maintained for about 50 days until increasing high concentration of nitrate production was found in the reaction and the NRR began to go down. The reason for this phenomenon can be attributed to the failure of anammox bacteria to compete NO_2^--N for substrate with NOB. As a result the concentration of ammonia was also increased and led to much worse nitrogen removal rate. Afterwards, even though AR was increased to 2.0L/min and ammonia concentration deceased, the concentration of nitrate continued increasing, which caused much lower NRR of 47%.

4. Conclusions

(1) Under this experiment condition, when DO concentration was kept as 0.13mg/L or AR was set as 1.60L/min, the optimum NO_2^--N/NH_4^+-N ratio can be achieved and long-term maintained.

(2) By adjusting AR, the one-stage anammox was achieved and the maximum nitrogen removal rate was gained when AR was kept as 150L/min.

Effect of Substrate Concentration on the Operation Performance of Anammox Process in a UASB Reactor

○Haiyuan MA[1], Shilong HE[1], Yuyou LI[1]*

Department of Civil and Environmental Engineering, Tohoku University, Japan
*E-mail: yyli@epl1.civil.tohoku.ac.jp

Abstract

This study investigate the effect of substrate concentration on the operation performance of Anammox process in a UASB reactor. The TN concentration was raised from 300mg/L, to 450mg/L and finally to 700mg/L. Under the condition of TN 300mg/L(nitrogen loading rate of 2.4kgN・d^{-1}・m^{-3}) and 450mg/L(nitrogen loading rate of 3.6kgN・d^{-1}・m^{-3}), the removal efficiency of TN reached 85.5% and 84.4%, respectively. When TN was raised up to 700mg/L, the average removal efficiency for TN dropped to 66.4%. The reason for removal efficiency decline is considered to be FA and FNA inhibition.

Keyword: Anammox, UASB, substrate concentration, FA, FNA

1. Introduction

In order to prevent the eutrophication of water environment, it's very important to remove nitrogen form waste water. Anaerobic ammonium oxidation (Anammox) is now a very attractive denitrogenation technique because it reduces the aeration cost and the need for carbon resource compared with the old process. In our research, continuous experiment was operated in a UASB reactor and the total nitrogen concentration was increased during three stage. The effect of substrate concentration on the operation performance of Anammox process in a UASB reactor was studied.

2. Materials and methods

2.1 Reactors and procedure

The reactor used in this research was shown in Fig.1. The effective volume of the reactor is 5L, and the temperature of the reactor was maintained in 33±1℃ by waterjacket. The inoculate sludge in this research is the granular sludge cultivated in our lab. The input synthesis substrate contains $(NH_4)_2SO_4$ and $NaNO_2$, and the mole ratio of NH_4^+:NO_2^- is 1:1.32. The condition of each period is shown in Table 1.

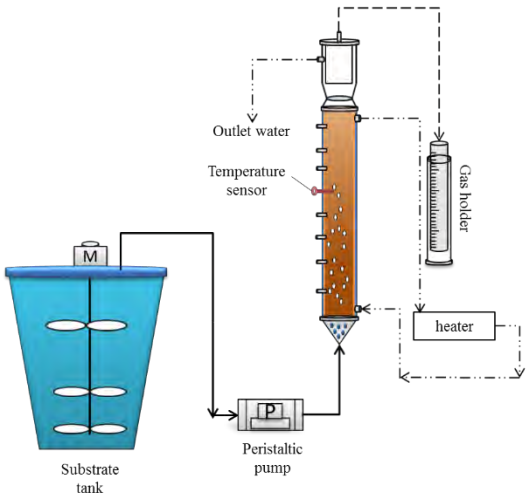

Fig. 1 the schematic of experiment

Table 1 the operation condition in each period

period	I	II	III
operation time(d)	1-76	77-111	112-219
HRT(h)	3	3	3
TN(mgN・L^{-1})	300	450	700
NLR(kgN・d^{-1}・m^{-3})	2.4	3.6	5.6

2.2 Analytical method

The water quality of input and output was measured every two days. The NO_2^--N and NO_3^--N were measured with the Agilent 7100 capillary electrophoresis system. The NH_4^+ was measured according to the standard methods (APHA, 2005). pH was measured with a pH meter and the nitrogen gas produce rate was measured with a gas holder everyday. The FA (free ammonia) and FNA (free nitrite acid) was calculated according to the formula below.

$$FA = \frac{17}{14} \times \frac{[NH_4^+ - N] \times 10^{pH}}{e^{[6344/(273+T)]} + 10^{pH}}$$

$$FNA = \frac{46}{14} \times \frac{[NO_2^- - N]}{e^{[-2300/(273+T)]} \times 10^{pH}}$$

The activity test was conducted with the sludge taken from 13cm, 33cm, 53cm height and cultivated in a 33℃ thermostatic water bath oscillator. The ongoing change of gas produce volume and the water quality were measured.

3. Result and discussion

3.1 Performance of continuous experiment

The ongoing change of gas produce rate, nitrogen removal ratio and nitrogen component is shown in Fig.1. In this research, the total nitrogen (TN) concentration was raised up from 300mg/L to 450mg/L and finally to 700mg/L under the HRT of 3h. Under the TN concentration of 300mg/L and 450mg/L, the removal ratio of NH_4^+-N is over 95%, and the TN removal ratio is 85.5% and 84.4%, respectively. Nevertheless, when TN is raised up

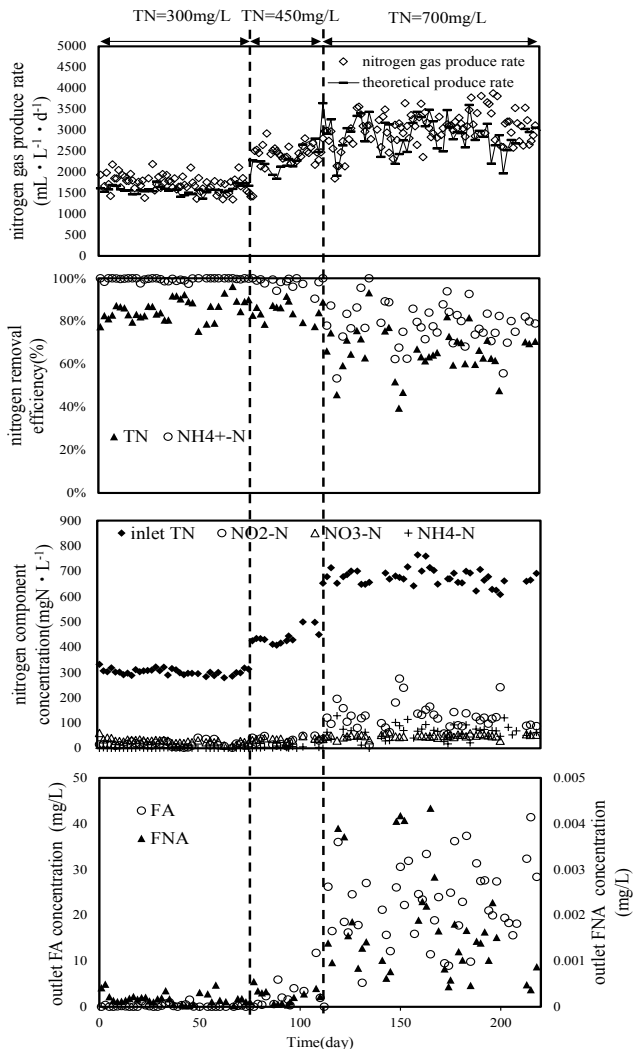

Fig. 2 ongoing change of continuous experiment

to 700mg/L, the removal of nitrogen came into a very unstable status. With about 100d continuous operation, the average removal efficiency is about 66.4%.

3.2 The inhibition of Anammox activity

The microorganism shows a severe variation according to the height as UASB reactor is an incompletely mixed reactor. The nitrogen component according to height is shown in Fig.3. The concentration of NH_4^+-N and NO_2^--N declined and the concentration of NO_3^--N rose. The result of the sludge activity test in this period is shown in Fig.4. The highest activity reached 0.513 gN・gVSS^{-1}・d^{-1} for the bottom sludge under TN 232mg/L. Nevertheless, when the TN is higher than 232mg/L, the Anammox activity was inhibited, and showed a dropping toward. The sludge taken from middle part and top part showed the same toward, and reached their highest activity between TN232-464mg/L. Furthermore, the activity of the sludge taken from middle part and top part only reached 18.4% and 11.0% of that of the bottom sludge.

As was shown in Fig.3, under the condition of TN700mg/L, the sludge in the whole reactor is under the TN of 232mg/L and the Anammox reaction was possibly inhibited. On the other hand, even low concentration of FA or FNA will inhibit the Anammox activity. According to the research result in our lab[1)], for granular Anammox sludge, when FNA is higher than 0.007mg/L or FA is higher than 20mg/L, 40% of the activity will be inhibited. From the continuous experiment, the FA and FNA of outlet water rose notably when TN

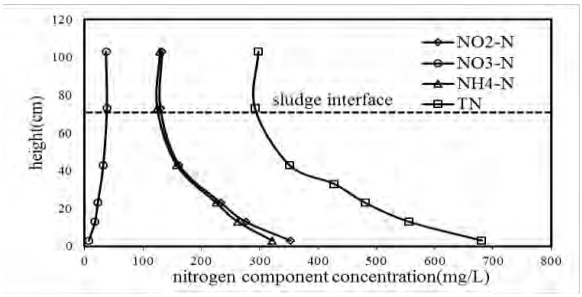

Fig. 3 nitrogen concentration variation according to height under inlet TN of 700mg/L

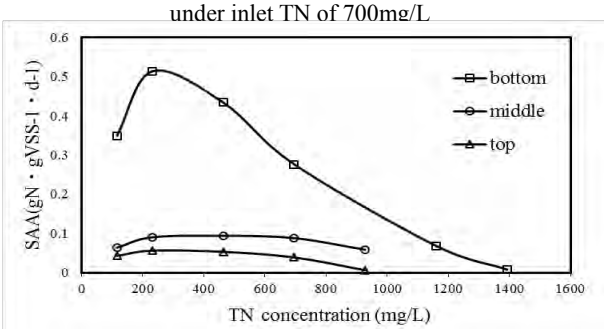

Fig. 4 specific activity of sludge from each part

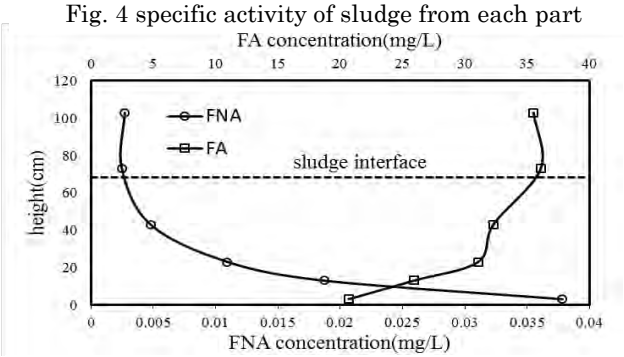

Fig. 5 FA and FNA variation according to height

is 700mg/L. The variation of FA and FNA according to height in this condition is shown in Fig.5. The FNA was over the inhibition concentration of 0.007mg/L below the height of 23cm, and the FA was over the inhibition concentration of 20mg/L. And because the sludge below the height of 23cm held high activity, we considered that FNA inhibited the removal efficiency of the whole reactor.

4. Summary

In this research, the TN concentration in a UASB Anammox reactor was raised from 300mg/L, to 450mg/L, and finally to 700mg/L. The following conclusion is obtained.

1) Under the condition of TN 300mg/L and 450mg/L, Anammox process is operated stably. In the nitrogen loading rate of 2.4kgN・d^{-1}・m^{-3} and 3.6kgN・d^{-1}・m^{-3}, the NH_4^+-N removal efficiency is over 95% and the removal efficiency of TN reached 85.5% and 84.4%, respectively.
2) When TN was raised up to 700mg/L, because of the inhibition of FA and FNA, the average removal efficiency for TN and NH_4^+-N is 66.4% and 78.8%, respectively.

It is very important to keep the inlet TN concentration under 450mg/L to prevent inhibition caused by FA and FNA in the UASB Anammox process.

References

1) ZHANG Yanlong, NIU Qigui, LI Yuyou, J. JSCE, Ser. G (Environmental Research) Vol.69, No.7, III515-III522, 2013

Current state of knowledge of antibiotics in the environment: a global approach

○Adriana Ledezma Estrada[1,2], Lu Xueqin[1], Yu-You Li[1,]

[1]Graduate School of Engineering, Tohoku University, Sendai 980-8579, Japan
[2]Escuela Nacional de Ciencias Biologicas del Instituto Politecnico Nacional. Av. Plan de Ayala S/N. Del. Miguel Hidalgo. Mexico City, Mexico
*E-mail: adriana@epl1.civil.tohoku.ac.jp

Abstract

Antibiotics first considered as the most important drugs to save lives now are in the list of emerging pollutants that threat life. This is the result of decades of misuse and overuse that has lead into a big problem of antibiotic resistance of pathogenic strains. In the last decade, due to the advance in science and the emerging concern on environmental topics, a deeper analysis of problem has been possible. Nowadays, the effect of the antibiotics in the environment is holistically approached. The influences of the economy, culture, biological, genetic and chemical processes are considered. On the other hand, the global concern has exerted a positive pressure to write stricter laws that demand not only a control in its use but its disposal. The result is an active development of new technologies to address this problem.

Keywords: antibiotics, antibiotic resistance, antibiotic environmental impact

1. Introduction

Although the first antibiotic was discovered 80 years ago it was during the World War II they were intensively used. In this period different kind of antibiotics were discovered and its use was diversified. Originally they were restricted to humans, but soon it was extended to agriculture i.e. live stock and cultivated land.

Initially the regulation was focused only in the toxicity due to the lack of knowledge about other side effects. It resulted in their misuse and abuse with significant consequences. By 1955 the 13% of *Staphylococcus aureus* (SA) were resistant to penicillin, in 1988 the resistance increased up to 93%, and nowadays almost any antibiotic can kill the Multi-Resistant *SA* (MRSA).

The presence of antibiotics in the environment was unknown and ignored because of their low concentration and ignorance on antimicrobial resistance. Today the advances in science have changed the perception of this global concern leading to stricter laws that consider not only its use but production and total elimination.

The last is a hot research in wastewater because most of the antibiotics and the resistant strains are spread in the environment by this means.

2. Global trends of antibiotics human consumption

The consumption of antibiotics is influenced by the countries' economy. Opposite to developed countries, developing countries have higher human consumption due to the low hygiene conditions that promote infectious diseases. However, for farming the use or abuse is almost the same. **Fig. 1** shows the growth of antibiotics consumption (AC) of 63 countries (doses per month) during the last decade (2000-2010). Most European countries have lowered the AC because of strict laws that limit its use only to absolute necessary cases and the trend is scaling to the farming sector. Most developed countries show a strong decrease in their AC. except for Australia and New Zealand that increased their AC. The decrease of AC could be ascribed to the calling for stricter laws to control the self-prescription in almost every country.

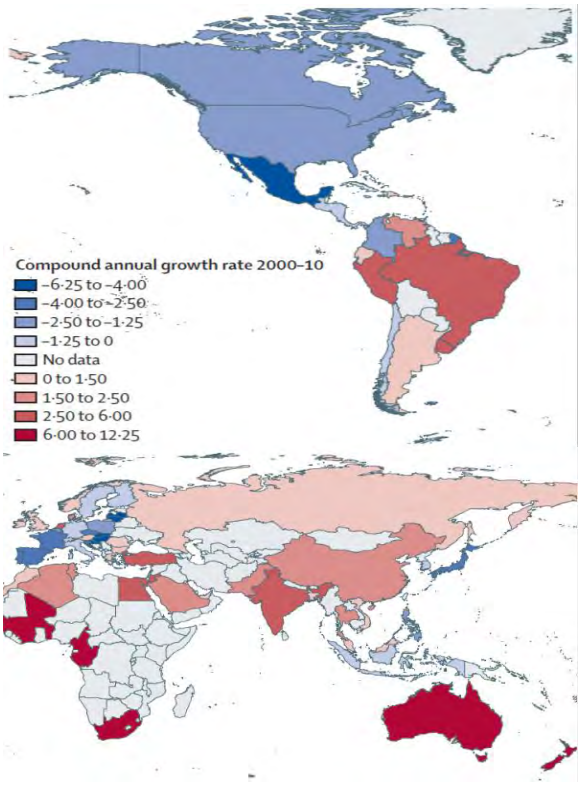

Fig. 2 Growth (decrease) rate of antibiotics consomptuin for 63 countries for the period between the years 2000 and 2010. Expressed as number of doses per month (Based on Van Boeckel et al., 2014).

3. RESISTANT MECHANISM

Antibiotics are naturally produced by microbes in the environment; the purpose of such antimicrobial substances is to protect them from other microbes that threat their existence. However, as a response the attacked microbes switch on genes, known as antibiotic resistant genes (ARGs), that encode for metabolites to protect them like enzymes which deactivate the antimicrobial substances.

Usually the resistance occurred after the microbes are in contact with the antibiotic whether at low concentrations or short time of exposure. Then, this resistance could be transferred to other microbes that had not been exposed to the antibiotic by means of horizontal genetic exchange of resistant elements. As a result, the antibiotic resistance is spread into other bacteria. For instance, Liu et al. reported that one bacterium can encode 8 different resistant genes while exposed to a single kind of antibiotic. This fact could explain the presences of multi-resistant antibiotic strains. Also this study confirms the horizontal transfer of the genetic material.

4. HEALTH IMPACT

Human health has been notably affected by the antibiotics. The lifespan was elongated and many lives were saved. However, it is improper use has also brought negative effects. The most important and best documented is the antibiotics resistance of pathogenic bacteria, which consequences are high mortality from common infections that can be treated. In the livestock has been notice that antibiotics put weight on, such effect is believed to boost human obesity. **Fig. 2** compares two farmed chickens, one in 1950 and the other in 2008.

Fig.2 Comparative weight gain of two chickens, on the left is without using antibiotics as growth promoters while the right is fed on antibiotics.

The recent cutting edge project of the human gut, has pointed out the important relationship of the microbes in the gut with the immunological system. A remarkable finding is that after taking antibiotics people are more prone to get another infection disease from different microbe including viruses.

Finally, the last founded antibiotics were synthetic and highly toxic. Therefore, the pharmaceutical industry since 2000 had nearly stopped the research on new antibiotics.

4. ENVIRONMENTAL IMPACT

The main impact on the environment is the slowly modification of the ecosystem that alters the trophic net, a process which eventually will affect human`s wellness. In agriculture sometimes antibiotics are used to protect the crops from plagues, like in apple or pear trees from *Erwina amilovora* also nown as fire blight.

Nevertheless, a particular concern is water pollution because it functions as a vector to transport resistant bacteria as well of ARGs to different places. Thus, the resistance is dispersed in big areas through the water natural flow; reaching also the soil and the air. Consequently, multi-resistant bacteria are more alike to appear even in pristine places. When the bacterial composition in the soil changes the plants that use to grow on it change as well. Then, the animals that depend of such vegetation will may face food scarcity and eventually some of them will disappear if they cannot adapt. This slow effect is scaled up until reach humans. Finally, another factor that promotes the dissemination of resistance are migration movements from animal but also from people traveling far from its original place because they could transmit the local or natural resistance to far places.

5. STAY OF THE ART:

The advances in analytic chemistry allow to detect and to measure antibiotics and other small related molecules in the environment, especially in water. Furthermore, genetics have also advanced and become more accessible thus more research on the microbial mechanism for the resistance had been achieved. The result of this knowledge has stressed: the importance of efficient wastewater treatments (WWT) to completely remove such kind of pollutants, and the creation of stricter laws to regulate its use. In the field of WWT new technology is been developed like the Advanced Oxidation Processes (AOPs), that completely oxidize such substances, efficient filtration processes to remove them or effective biological process like membrane bioreactors MBRs are tried.

Additionally, this problem is approached through better regulations and educational campaigns to explain the problem and create conscience. In Europe this movement is very strong and is gaining territory around the world. Still, there is so much to do but the solution is on the way.

6. CONCLUSIONS

Antibiotic resistance is an environmental-health problem recently consider as a significant threat for human health. Years of indifferences have buildup remarkable problems difficult to address. However, since it is a global concern strong actions are taken. To overcome this challenge broad research on this topic as well deeper understanding is needed..

7. References

1. Miaomiao Liu, et. al. Abundance and distribution of Macrolide-Lincosamide-Streptogramin resistance genes in anaerobic-aerobic system treating spiramycin production wastewater, Water Research, 63 (2014) 33-41
2. Thomas P Van Boeckel, Sumanth Gandra, Ashvin Ashok, Quentin Caudron, Bryan T Grenfell, Simon A Levin, Ramanan LaxminarayanGlobal antibiotic consumption 2000 to 2010: an analysis of national pharmaceutical sales data. The Lancet. 14 (2014) 742-750
3. Heather K. Allen, et. al. Call of the wild: antibiotic resistance genes in natural environments. Nature Reviews: Microbiology focus on antimicrobial resistance 8 (2010) 251-259

Phase Separation by Hyper-thermophilic Temperature in Anaerobic Digestion of Waste Activated Sludge

○Yu QIN[1], Lijie WU[2], Atsushi HIGASHIMORI[2], Toshimasa HOJO[2], Yu-you LI[2]

[1] Graduate School of Environmental Studies, Tohoku University, Sendai 980-8579, JAPAN
[2]Graduate School of Engineering, Tohoku University, Sendai 980-8579, JAPAN
*E-mail: yyli@epl1.civil.tohoku.ac.jp

Abstract

In order to investigate the performance of phase separation by different temperatures as first stage in a temperature phased anaerobic digestion (TPAD), continuous experiments were conducted combining a thermophilic (55˚C) first stage and a mesophilic (35˚C) second stage, named TM-TPAD, and then combining a hyper-thermophilic (70˚C) first stage and a mesophilic (35˚C) second stage, named HM-TPAD, focusing on the long-term performance, organic degradation and particle hydrolyzation. The experiments of a single mesophilic (35˚C) anaerobic digestion (MAD) were also carried out as comparisons. In this study, the HM-TPAD was operated stably in the long run, achieving a volatile solids (VS) destruction of 51.8%, which was 1.16-fold and 1.39-fold of the values of TM-TPAD and MAD respectively. It can also be concluded that the higher temperature is set to the first stage, the more efficient organic degradation and particle hydrolyzation is obtained for WAS digestion. Especially, the acidogenic phase and methanogenic phase were separated in the first stage only when it was operated under hyper-thermophilic (70˚C) condition in the hydraulic retention time of 6 days.

Keywords: Anaerobic digestion, Temperature phased anaerobic digestion, Hyper-thermophilic, Waste Activated Sludge

1. Introduction

Nowadays expensive cost has to be spent on disposing the sewage sludge from wastewater treatment plants. Anaerobic digestion can minimize those organic solids and reuse the produced biogas as fuel, which is also an effective method to ease the urgent problems of shortage of fossil fuels and global warming. Practically, most of the anaerobic digesters were set at the mesophilic temperature of 35˚C. Through the mesophilic anaerobic digestion of sewage sludge, which consists of primary sludge and waste activated sludge (WAS), the latter was confirmed slower to degrade. Furthermore, hydrolysis was reported as the rate-limiting step along the methane fermentation.

In the recent decades, hyper-thermophilic condition attracts great interests in the field of anaerobic digestion of solid wastes. Due to the effect of physical denaturation from heating and the rapid reaction from the functioning enzymes, the hyper-thermophilic conditions of 70˚C have been reported capable to evaluate the degradation of WAS. On the other hand, most of the lab-scale hyper-thermophilic digesters were focused on acidogenesis or hydrogen fermentation and the methanogenic archaea communities were reported fragile and unstable under hyper-thermophilic conditions. Thus, we connected a mesophilic digester following the hyper-thermophilic tank, which guarantees a stable environment for methane fermentation.

Temperature phase anaerobic digestion (TPAD) has also been extensive studied for its effectiveness on the phase separation. By separating the acidogenic phase and the methanogenic phase, each phase provides better condition for its dominant microbial communities. Whereas, compared to numerous reports on TPAD applied with thermophilic (55˚C) and mesophilic conditions, hyper-thermophilic conditions have rarely been reported in TPAD.

In this case, this study was proposed to investigate a TPAD combining hyper-thermophilic (70˚C) and mesophilic (35˚C) conditions (HM-TPAD) focusing on its long-term performance and organic removal efficiencies. As comparison, a TPAD combined with thermophilic (55˚C) and mesophilic conditions (TM-TPAD) and a single-phase mesophilic anaerobic digestion (MAD) were also operated.

2. Experimental apparatus

The apparatus were as shown in **Fig. 1**. The total hydraulic retention time (HRT) for each process was 30 days.

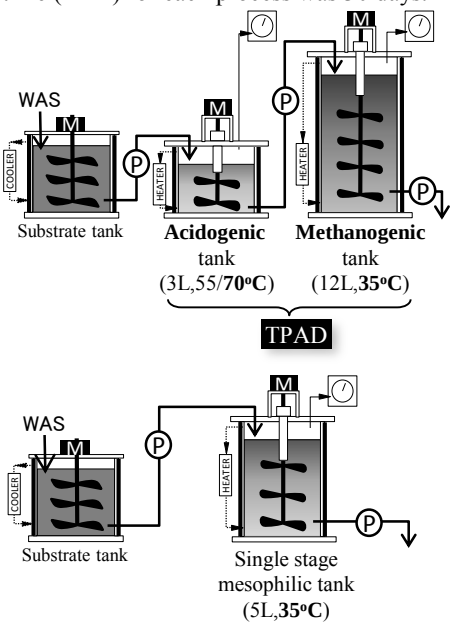

Fig.1 the schema of the experimental apparatus

The HM-TPAD were started right after the TM-TPAD by resetting the temperature in acidogenic tank from 55˚C to 70˚C. The results and discussion were based on the steady stage of each conditions, i.e. after the duration longer than 90 days (3 times of HRT).

3. Results and discussion

The performance of TPAD were as shown in **Fig. 2**. In the acidogenic tank of TM-TPAD, gas production rates were obviously high and methane took about 60% in the biogas. The pH values around 7.5 and little accumulation of volatile fatty acids (VFA) in this tank suggested that the methanogenesis was remained and active in the acidogenic tank. When the acidogenic tank changed to hyper-thermophilic temperature, gas production rate was relatively low and methane took only 40% in the biogas. The sharp decrease of pH until around 6.5 and increase of VFA concentrations implied that methanogenesis was weak in this tank. However the acidogenic tank performed, the methanogenic tank remained at pH values around 7.5 and no VFA detected. The stable performance of methanogenic tank ensured the favor environment for methanogenesis and the safeness of the whole TPAD process.

The organic removal efficiencies in each process are calculated by the following formula and shown in **Fig. 3**.

$$\text{Removal (\%)} = \frac{c_{\text{influent}} - c_{\text{effluent}}}{c_{\text{WAS}}} \times 100\%$$

The removal efficiencies for each process ranked as HM-TPAD > TM-TPAD > MAD, which intimated the tendency that the higher temperature applied in the acidogenic tank, the more enhancement obtained through the whole process. The volatile solids (VS) removal of HM-TPAD was 51.8%, which was 1.16 times and 1.39 times of the values of TM-TPAD and MAD, respectively.

Referring to the distributions of organic removal efficiencies between acidogenic and methanogenic tanks, the former degraded more than latter in TM-TPAD while on the contrast acidogenic tank degraded less in HM-TPAD. Even though the hyper-thermophilic acidogenic tank achieved less removals compared to TM-TPAD, it was suggested that the higher temperature resulted the proteins, which is the main component of WAS, denatured to be more degradable in the following methanogenic tank.

In order to grasp the degrading behavior of each process, the COD balances were calculated and shown in **Fig. 4**. 100% was the total COD values of the substrate WAS.Both the TM-TPAD and HM-TPAD left less particle COD (solids) than single phase MAD, especially the HM-TPAD reduced 15% more solids than MAD. The soluble COD, which mainly contained undegradable components, took up about 10% of the total COD. The major amounts of methane was produced in acidogenic tank of TM-TPAD while produced in methanogenic tank of HM-TPAD. Only 5% of COD were transformed into methane in acidogenic tank of HM-TPAD suggested that the phase separation were achieved, which is considered the reason for higher degradation ratio for HM-TPAD.

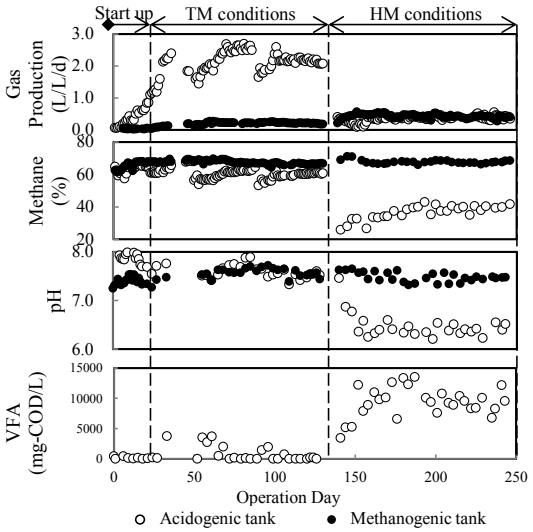

Fig. 2 Long-term performance of TPAD

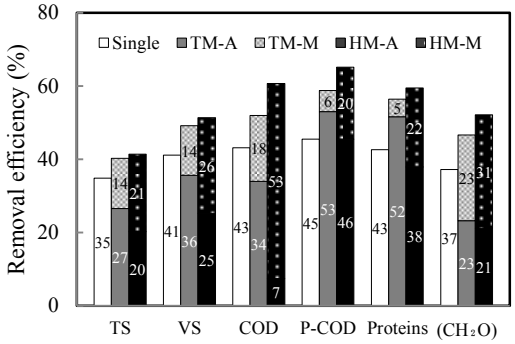

Fig. 3 Removal efficiencies in each process

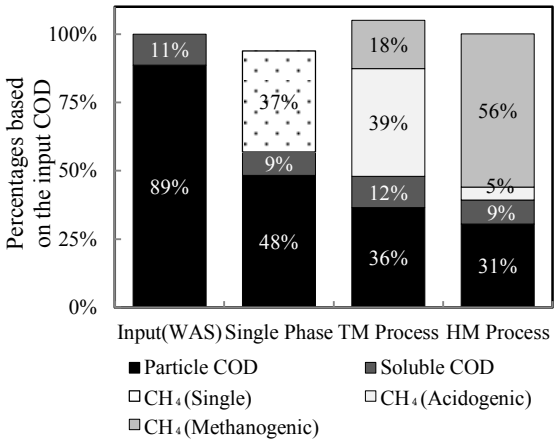

Fig. 4 COD balance of each process

4. Conclusions

1) The TPAD was operated stably in the long run under TM and HM conditions;

2) The higher temperature is set to the first stage, the more efficient organic degradation and particle hydrolyzation is obtained for WAS digestion. HM-TPAD achieved the volatile solids (VS) destruction of 51.8%, which was 1.16-fold and 1.39-fold of the values of TM-TPAD and MAD respectively;

3) The acidogenic phase and methanogenic phase were separated in the first stage only when it was operated under hyper-thermophilic (70˚C) condition in the hydraulic retention time of 6 days.

Session II

Special lecture

River Discharge Variations Attributed to Extreme Rainfall in Oman

○Luminda GUNAWARDHANA[1]*, Ghazi AL-RAWAS[2], So KAZAMA[3]

[1,2]Department of Civil and Architectural Engineering, Sultan Qaboos University, Oman
[3]Graduate School of Environmental Studies, Tohoku University, Sendai 980-8579, Japan
*E-mail: luminda@squ.edu.om

Abstract

This study investigates how the extreme precipitation and subsequent wadi flow are affected by climate change in an arid catchment area in Oman. A lumped-parameter rainfall-runoff model and 6-member ensembles of General Circulation Models from the Coupled Model Intercomparison Project Phase 5 (CMIP5) were used to simulate the wadi flow response to variation in precipitation. Yearly maxima of the daily precipitation and wadi flow for varying return periods were compared by fitting the Generalized Extreme Value distribution function. The results indicate that extreme precipitation events consistently increase by the middle of the 21st century for all return periods (49-52%) but changes may become more profound by the end of the 21st century (81-101%). Consequently, the relative change in extreme wadi flow is greater than twofold for all of the return periods in the late 21st century compared to the relative changes that occur in the mid-century period.

Keywords: Climate change, weather generator, frequency analysis, Oman

1. Introduction

An expanded body of evidence, along with the physical explanation by Trenberth et al. (2003), supports the conclusion that the global warming driven by both natural and anthropogenic emissions of greenhouse gases increases mean global precipitation (Cubash and Meehl, 2001). Karl and Trenberth (2003) demonstrated that, as the temperature and the associated water-holding capacity of the atmosphere increases, the frequency of extreme daily precipitation increases, even when total precipitation remains constant. The Fifth Assessment Report (AR5) of the United Nations Intergovernmental Panel on Climate Change (IPCC) concluded that further increase in anthropogenic greenhouse gas concentrations will cause irreversible changes in the climate system on centuries-long time scales. Based on the projections of three of the four emission scenarios (Representative Concentration Pathways commonly known as RCPs) considered in IPCC AR5, the rise in the mean global surface air temperature by the end of the 21st century relative to the pre-industrial period is likely to exceed 1.5°C (Symon, 2013). Consequently, the intensity of extreme precipitation events is expected to increase in many parts of the world (Kharin et al., 2007)

Arid and semi-arid areas, where conditions of chronic water stress, catastrophic flooding and prolonged drought prevail, such as in the Gulf region of the Middle East, are particularly vulnerable to the impacts of extreme climate events. Gunasekara et al. (2013) analyzed the combined impacts of population change and climate change and identified the Middle East as one of the four regions that will be exposed to extremely negative impacts that could lower fresh water availability by 50% by 2100 compared to the situation in 2000. In Oman, changes in precipitation and temperature extremes are already evident and have caused an accelerated frequency of flooding (Al-Rawas and Valeo, 2010). However, a comprehensive analysis to determine the potential impacts of climate change on precipitation and the water cycle has not yet been conducted for Oman. This study, to the best of our knowledge is the first of its kind for Oman. The results from 19 RCP scenarios embedded in 6 state-of-the-art global climate models from the Coupled Model Intercomparison Project Phase 5 (CMIP5) were used to simulate the present-day extremes in precipitation and wadi flow and to project their potential changes in the future in the Al-Khod catchment area in Muscat, the capital city of Oman.

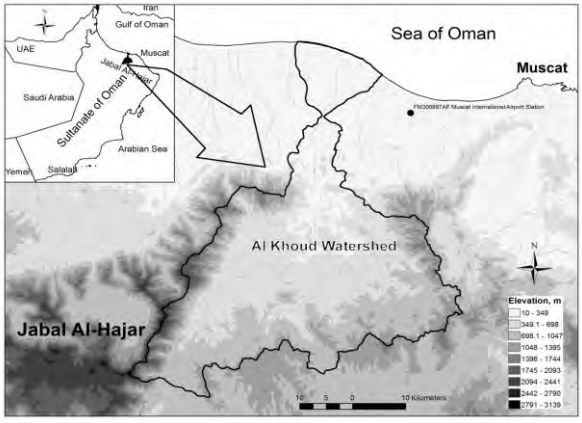

Fig. 1 Study area

2. Study Area

Oman is located in the southeastern corner of the Arabian Peninsula (Fig. 1). It covers an area of 309,500 km^2 and encompasses a diverse range of topography, including mountain ranges, arid deserts and fertile plains. The climate varies mainly from semi-arid to hyper-arid. On average, the annual rainfall is less than 100 mm, compared to the global annual mean of 1123 mm. The Al-Khod catchment encompasses a total area of greater than 1600 km^2. Because of the common flash floods that occurred in this wadi, Al-Khod dam was built at the downstream end of the catchment to prevent flooding.

3. Methodology

The Tank Model used in this study to simulate rainfall runoff process is a lump-parameter model that was first developed by Sugawara (1995). The ephemeral flows (rain-dependent flows) that occur in arid areas such as Oman only endure intense water runoff for short periods; hence, the evapotranspirative effect on wadi flow was neglected for this extremely short duration of the year.

Predictions of future climate require the generation of a plausible range of greenhouse gas (GHG) emission scenarios and the simulation of earth system responses to the corresponding emissions. In this study, we employed 6 GCMs and 4 scenarios, which altogether produced 19 scenarios to evaluate precipitation-driven changes in wadi flow in the Al-Khod catchment. Based on the data availability for our study area, the years 1977-2005 were selected to represent the past climate. Two future periods, each encompassing 20 years, were also defined: 2040-2059 and 2080-2099. Even though many models included in the CMIP5 have improved model resolutions, the horizontal resolutions of GCMs are still modest and generally too coarse to apply directly to local-scale impact studies. We used LARS-WG5.5 (Long Ashton Research Station Weather Generator, version 5.5), a widely used stochastic weather generator (Semenov and Stratonovitch, 2010), to downscale GCM precipitation records to the local scale. Moreover, the yearly maxima of the daily precipitation and the wadi flow were analyzed using the Generalized Extreme Value (GEV) distribution function.

4. Results and Discussion

The Tank model performance was evaluated using precipitation and wadi flow events from 1997 to 2011. Considering the availability of quality data and the ephemeral nature of the wadi flow, 17 discrete hydrographs were selected. The overall model efficiency was estimated to be reasonably high as indicated by a NSE of 0.79.

We found a significant increase in extreme precipitation in base period. The contribution from very wet days (R95P) to the annual precipitation (PRCPTOT) shows steady raise (Fig. 2), even though its trend is significant at 75% only.

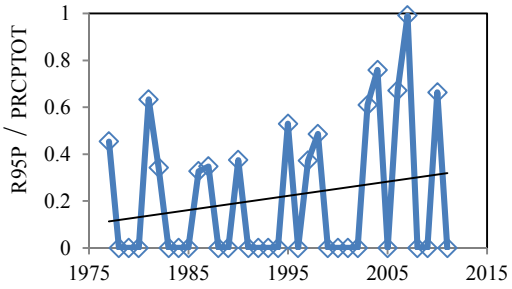

Fig. 2 Trend of extreme precipitation

Our results of the annual maximum precipitation for the various return periods indicate that, for small return periods (e.g., 5 and 10 years), the projected range of the change is relatively smaller. As the return period increases (e.g., 20 and 50 years), the projected range of the change becomes relatively large. For example, the projected range between the maximum and minimum extreme precipitation is 75 mm for the 5 year return period for 2080-2099 and the range increases to 218 mm for the 50 year return period. A very similar phenomenon occurs for the 2040-2059 time period as well. When the mean of all the scenarios was considered, the extreme precipitation for the different return periods consistently increases relative to the estimations for the present climate. Notably, these increases are greater for the 2080-2099 period compared to the corresponding changes in the 2040-2059 period. For example, the relative change in the extreme precipitation for the 20 year return period is 49% for the 2040-2059 period and increases to 83% for the 2080-2099 period. On average, the relative increase in the magnitude of extreme precipitation for all the return periods is 51% (ranging between 49% and 52%) for the 2040-2059 period and 89% (ranging between 81% and 101%) for the 2080-2099 period.

A similar effect is also expected for changes in wadi flow. Figure 3 presents a boxplot of the annual maximum wadi flows for the various return periods. Similar to the extreme precipitation, the projected range of the change is smaller for the small return periods and, as the return period increases, the projected range of the changes in extreme wadi flow become substantial. The annual maximum wadi flow consistently increases in the mid and late century with a significantly greater increase towards the end of the 21st century. For example, when the means of all the scenarios and return periods were considered, the extreme wadi flow increases between 18% and 43% for the 2040-2059 period and between 54% and 84% for the 2080-2099 period across all return periods compared to the estimated mean wadi flow for the present climate. Notably, for all return periods, the relative change in extreme wadi flow is more than twofold greater in the late 21st century compared to the relative change in mid-century.

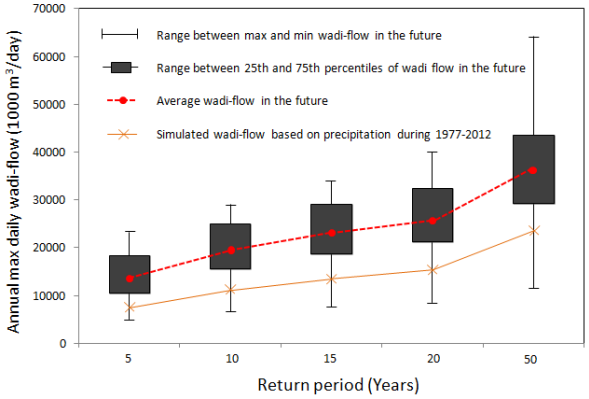

Fig. 3 annual maximum wadi flows for the various return periods for 2080-2099.

5. Conclusions

Our results indicate that the magnitude of precipitation during extreme events will significantly increase by the middle of the 21st century and become even more intense by the end of the 21st century.

The ratio between the relative change in wadi flow and the relative change in precipitation is always greater for the late-century period compared to the mid-century or present climate periods. Therefore, the increase in intense extreme precipitation projected in future will likely cause extreme wadi flows beyond the precipitation and associated wadi flow response observed for the present climate.

A field-scale observation method for non-point source pollution of paddy fields

○Baolin SU[1,*], Ningbo HUANG[1], Ruirui LI[2]

[1]College of Water Sciences, Beijing Normal University, Beijing 100875, China
[2]School of Environment, Tsinghua University, Beijing 100084, China
*E-mail: subl@bnu.edu.cn

Abstract

This paper proposes a direct method to observe NPS pollution from paddy fields. The evapotranspiration and infiltration loss hydrographs of paddy fields in different stages of growing season are estimated firstly depended on observed water-depth, rainfall and irrigation data, and outflow of paddy fields is analyzed through water balance approach. Combined with observed surface water quality data, loads of NPS pollution in outflow from the paddy field can be derived. The proposed method can be applied to quantificational observation of NPS pollution from paddy field in the condition of multi-outlets and dynamic variation of the lowest ridge height during growing season, which is impossible to conduct field observation by using conventional methods.

Keywords: non-point source pollution, runoff observation, paddy field, evapotranspiration and infiltration loss

1. Introduction

Currently, there are two ways to observe non-point source pollution which are Runoff Storage Pond method (RSP) and Synchronous Observation (SO) method of water quantity and quality. For RSP method, it is necessary to construct a runoff pond with specific volume at the outlet of a paddy field, and total generated runoff and pollutant loads during a rainfall event will concentrate into the pond, and runoff volume and concentration can be measured. Although the RSP method has been applied for many cases, there are some limitations. Firstly, there are some pre-conditions for applying RSP method, such as runoff storage ponds with certain volume, and unchangeable ridge height of unique outlet. In the field observation, these pre-conditions are quite difficult to meet. There is more than one outlet for most paddy fields, and the ridge height of each outlet is variable due to water management during growing period. Secondly, if the experimental field is very large, the big pond volume is needed. But it is very hard, sometimes impossible to find a suitable space to construct a big runoff storage pond in the field.

The SO method measures water samples and outflow volume synchronously at a certain time interval when outflow or runoff generates. These data will be used to analyze runoff hydrograph and runoff quality variation. However, the SO method also need the experimental field have only one outlet and cannot consider the ridge height variation during whole growing season.

In order to solve above problems which conventional methods cannot be applied to conditions with multiple outlets and lowest ridge height variation, this paper proposes a new observation method, which estimates the evapotranspiration (E) and infiltration loss (F) during different growing periods based on observed water depth variation of paddy fields, and calculates outflow through water balance theory. Then, combined with surface water quality variation data, non-point source pollution load exported from paddy field can be estimated.

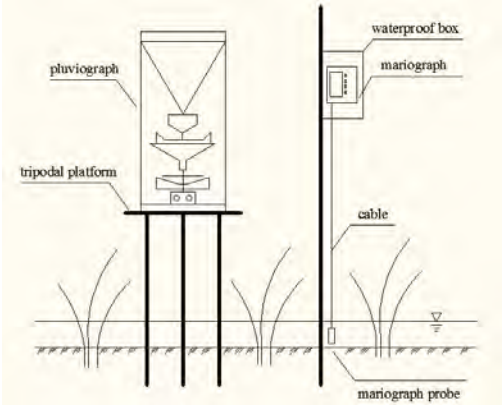

Fig. 1 Schematics of instrument installation

2. Materials and Methods

2.1. Instrument installation

A pluviograph (rain gage) and a mariograph (water level meter) need to be installed in the experimental field after paddy transplantation (Figure 1). The pluviograph should be installed on a fixed tripodal platform, and the rain barrel should be kept vertically and 70cm high from the ground. The mariograph was installed in the paddy field, and the mariograph probe should be installed at about 2 cm high above the field bottom to prevent probe from blocking by mud, and probe installation height should be kept unchanged during whole growing season.

2.2 Data collection

In order to observe continuously rainfall and water depth, pluviograph was set up to record rainfall every 10 minutes, and mariograph was set up to record surface water depth variation every 30 minutes. Meanwhile, different sampling points were selected in the experimental field to obtain average water quality of surface water at regular intervals. Surface water samples were collected twice a week in this study for water quality analysis in the laboratory. Additionally, it was also needed to investigate the water management practices such as the time and duration of irrigation and manually drainage.

2.3 Data analysis method

The monitored variables related to outflow estimation include rainfall, evapotranspiration, infiltration loss, irrigation and water depth variation. For each downstream paddy field, the water and nutrients in outflow will directly flow into surface water system, and thus forms the non-point source pollution. Water balance equation is shown as following:

$$P + R_{in} - (E + F) - R_{out} = \Delta H \quad (1)$$

Where P is daily rainfall (mm), R_{in} is irrigation water inflow (mm), E is evapotranspiration loss (mm), F is infiltration loss (mm), R_{out} is water outflow (mm), ΔH is depth variation (mm).

Normally R_{in} and R_{out} will not happen at the same time. ΔH can be observed through mariograph that indicates how P, R_{in}, $(E + F)$ and R_{out} affect water depth variations. Therefore, the parameter R_{out} can be calculated as following:

$$\begin{cases} \Delta R_i = P_i - (E_i + F_i) - (H_{i+1} - H_i) \\ \Delta R_i > 0, \quad R_{out,i} = \Delta R_i \\ \Delta R_i < 0, \quad R_{in,i} = -\Delta R_i \end{cases} \quad (2)$$

During raining period, $\Delta R_i > 0$ means that there is water left after the evapotranspiration, infiltration loss and surface water depth variation. For this portion of water, it flows out of the paddy field in the form of surface outflow. Therefore, the surface outflow can be estimated as ΔR_i. On the other hand, if $\Delta R_i < 0$, it means that the rainfall is not enough to supplement the change of water quantity. Therefore, irrigation was assumed instead of outflow, and the amount of irrigation can be estimated according to water balance.

The key point of this method is to decide the decreasing rate of water depth by analyzing water depth variation process when no outflow occurs. The outflow volume of non-point source pollution was calculated by the amount of decreased water volume deducting with evapotranspiration and infiltration loss (E+F).

3. Results and Discussion

3.1. Evapotranspiration and infiltration loss

The evapotranspiration and infiltration loss of paddy fields include surface water evaporation, plant transpiration and infiltration. The rate of water depth drops down stably and smoothly caused only by the loss of evapotranspiration and infiltration during no-rain, no-irrigation and no-artificially drainage periods (Figure 2).

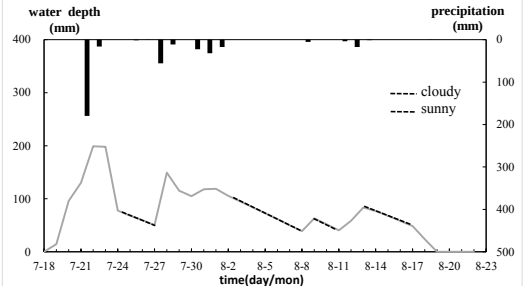

Fig. 2 Schematics of evapotranspiration and infiltration loss analysis

When estimating evapotranspiration and infiltration loss, sudden change periods of water depth should be avoided such as periods of rainfall, irrigation or artificially drainage. Thus, steady water depth decreasing periods in each rice growing stages and different weather conditions were chosen to calibrate and estimate the average evapotranspiration and infiltration loss (E+F) process, which can be used to calculate ΔR_i in Equation (2). The (E+F) estimates for different growing stages are shown in Table 1 and Figure 3. Thereinto, it is assumed that (E+F) are approximately equal to values with similar weather conditions as cloudy or sunny days depending on observed rainfall process and linear interpolations for periods of rainfall, irrigation or artificially drainage.

Table 1 Results of evapotranspiration and infiltration loss rate

Growing period		returning green	tillering	jointing -booting	maturity
Time duration		May 15~ Jun 6	Jun 7~ Jul 17	Jul 18~ Aug 22	Aug 23~ Oct 14
range of (E+F) (mm d^{-1})	overcast & rainy	4-6	6-8	8-10	7-9
	sunny	5-7	7-9	9-12	8-10

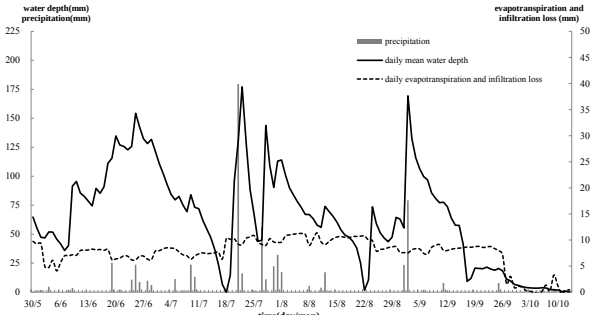

Fig. 3 Daily mean water depth, rainfall and evapotranspiration and infiltration loss hydrographs

3.2. Outflow estimation

As shown in the Table 2, the daily outflow from the experimental paddy field during the whole growing period can be calculated based on Equation 2.

As we can see from Table 2, there were totally 18 rainfall events in year 2012, and 11 events generated outflow and formed non-point source pollution. Besides, there were 3 times of rice fields drying processes (18/7, 22/8 and 16/9) which also caused non-point source pollution.

Table 2 showed that both heavy rainstorm (1 time) and storm rainfall (2 times) generated outflow. The rainfall of June 19th was 25.4mm but no outflow happened because there were 10 days in dry period before the rainfalls and the field was short of water. Moreover, there were 4 times of moderate rain, and 3 times of them generated outflow.

Table 2 Calculation results of outflow

No.	date(d/m)	rainfall (mm)	Water depth (mm)	(E+F) (mm)	Inflow (mm)	Outflow (mm)	Remarks
1	31/5	1.5	55.1	9.2			
	1/6	1.9	47.4	9.3	6.9		irrigation
	2/6	0.2	46.9	4.9	9.7		
	3/6	4.7	51.9	4.7			
2	8/6	2.1	40.2	6.9	56.2		irrigation
	9/6	3.5	91.5	7.2	7.7		
3	19/6	25.4	115.6	6.2			
4	21/6	2.3	127.0	6.5	3.0		irrigation
5	24/6	10.8	125.7	6.2	24.1		irrigation
	25/6	23.7	154.3	6.2		29.3	drainage
	26/6	8.8	142.5	6.9		12.2	
6	28/6	9.9	128.2	6.3			drainage
	29/6	6.1	131.8	6.2		10.0	
7	5/7	11.3	79.7	8.3			
8	7/7	1.4	75.2	7.2			
	8/7	1.3	69.5	7.0	20.3		irrigation
	9/7	23.7	84.1	6.3		28.2	drainage
	10/7	13.2	73.2	7.0		7.5	
9	14/7	0.0	47.4	7.4		2.6	
	15/7	0.0	37.4	7.5		6.1	drainage
	16/7	0.0	23.8	7.7		9.8	

No.	date(d/m)	rainfall (mm)	Water depth (mm)	(E+F) (mm)	Inflow (mm)	Outflow (mm)	Remarks
10	21/7	179.6	130.3	9.2		123.6	
	22/7	16.3	177.1	9.1		55.2	
	23/7	0.0	129.1	10.3		30.1	overflow
	24/7	0.0	88.6	10.6		10.3	
	25/7	1.3	67.8	10.9		14.3	
11	27/7	55.9	44.9	9.2	52.1		irrigation
	28/7	11.1	143.7	9.0		36.2	drainage
	29/7	0.0	109.7	10.3		9.1	
12	30/7	22.4	90.3	9.6	10.0		irrigation
	31/7	32.1	113.1	9.5		21.7	drainage
	1/8	17.3	114.0	9.6		20.9	
13	8/8	5.4	66.9	9.0			
14	11/8	3.9	55.9	9.7	23.9		irrigation
	12/8	17.2	74.0	9.1		12.3	drainage
	13/8	1.1	69.7	9.7	4.3		irrigation
15	20/8	0.0	38.3	10.7		2.4	drainage
	21/8	0.0	25.2	10.7		12.9	
16	1/9	23.5	55.4	7.6	98.0		irrigation
	2/9	79.2	169.3	7.5		108.4	drainage
17	6/9	2.0	99.7	7.4	2.6		irrigation
	7/9	0.3	96.9	7.3		4.3	drainage
18	11/9	8.0	77.6	8.0		3.7	drainage
	12/9	1.5	73.8	8.0		3.4	
19	15/9	0.0	57.6	8.4		7.7	drainage
	16/9	0.0	41.5	8.5		23.7	
20	25/9	7.9	20.4	8.0			
21	9/10	3.1	2.0	3.3			

3.3. Event Mean Concentration Calculation

Event Mean Concentration (EMC) is an average or "flow-weighted" pollutant concentration that is "representative" concentration for agricultural runoff from a particular land use. The EMC can be calculated as the total pollutant load from paddy filed outflow divided by the total outflow volume caused by a particular rainfall event and its values vary greatly between land uses and rainfall events.

In this study, Equation (3) is used to calculate EMC:

$$EMC = M/V = \int_0^t C_t Q_t dt \Big/ \int_0^t Q_t dt = \sum C_t Q_t \Delta t \Big/ \sum Q_t \Delta t \quad (3)$$

Where M is total pollutant load of outflow runoff, V is total runoff volume, t is time, C_t is the concentration of pollutants at time t, Q_t is runoff flow rate at time t, and Δt is sampling time interval.

According to Equation (3), we can calculate the EMCs of experimental paddy field for each rainfall event with outflow generation (Table 3).

Table 3 EMCs of target paddy plot during growing period

Date	Outflow (mm)	Concentration (mg/L)		Outflowed pollutant mass (mg/m^2)		EMC(mg/L)	
		NO_3-N	NH_4-N	NO_3-N	NH_4-N	NO_3-N	NH_4-N
25/6	29.28	1.85	4.42	54.17	129.42	1.85	4.43
26/6	12.20	1.84	4.45	22.46	54.31		
29/6	10.00	1.8	4.25	17.99	42.49	1.80	4.25
9/7	28.20	0.96	3.86	27.07	108.85	0.96	3.83
10/7	7.50	0.97	3.7	7.28	27.75		
14/7	2.56	1.22	4.87	3.12	12.46		
15/7	6.05	1.25	4.64	7.56	28.05	1.26	8.47
16/7	9.78	1.28	4.42	12.52	43.22		
21/7	123.60	0.99	4.25	122.36	525.30		
22/7	55.17	1.05	4.08	57.93	225.11		
23/7	30.09	1.1	3.9	33.10	117.35	1.04	5.25
24/7	10.26	1.16	3.73	11.90	38.27		
25/7	14.29	1.22	3.56	17.44	50.88		
28/7	36.20	1.39	3.04	50.32	110.06	1.38	3.05
29/7	9.07	1.34	3.07	12.15	27.83		
31/7	21.68	1.25	3.13	27.10	67.85	1.23	3.14
1/8	20.89	1.2	3.16	25.07	66.01		
20/8	2.42	2.74	3.74	6.63	9.05	2.84	3.78
21/8	12.87	2.86	3.79	36.80	48.76		
2/9	108.42	2.49	2.49	269.97	269.97	2.49	2.49
7/9	4.30	3.18	3.24	13.67	13.93	3.15	3.35
11/9	3.70	3.12	3.48	11.54	12.88	3.11	3.51
12/9	3.40	3.1	3.54	10.54	12.04		
15/9	7.67	3.87	3.71	29.70	28.47	4.06	3.76
16/9	23.69	4.12	3.77	97.60	89.31		
total				**985.98**	**2159.60**	1.66	3.64

4. Conclusions

(1) It is found that the decrease rate of water depth caused by evapotranspiration and infiltration loss is stable and well-regulated, and has close relations to meteorological condition and rice growing stages. Thus, the evapotranspiration and infiltration loss in different growing stages and meteorological conditions can be found out by variation of surface water depth, which is the most important step in this proposed method.

(2) Through observing the variation of water depth, and recording rainfall and paddy field water management practices, the evapotranspiration and infiltration loss (E+F) can be determined for different paddy growing stages. Then the runoff outflow process can be estimated by applying water balance approach.

(3) The proposed runoff observation method is more easily operable in observation of NPS pollution from paddy fields, especially in the condition when a paddy field has multi-outlets of outflow and lowest ridge heights varies through whole growing seasons which conventional observation methods fail to apply.

Algae as Energy Securing, Supplement Reserve and Formulating Carbon Sequestration for Waste Management from Palm Oil Mill Effluent (POME)

○Fadhil

Institute of Environmental Water Resources and Management (IPASA) c/o (WATER RESEARCH ALLIANCE)
Department of Environmental Engineering, Faculty of Civil Engineering, Universiti Teknologi Malaysia, 81310 Skudai Johore, Malaysia

*E-mail: mfadhil@utm.my

Executive Summary

Algae are defined as any organisms which are plant-like and perform photosynthesis. Based on their morphology and size, algae are typically subdivided into two major categories—macroalgae and microalgae. Microalgae are microscopic organisms that grow in salt or fresh water. The three most important classes of microalgae in terms of abundance are the diatoms (*Bacillariophyceae*), the green algae (*Chlorophyceae*), and the golden algae (*Chrysophyceae*). Growing algae on wastewater streams have a number of benefits. It will offset additional costs for nutrient removal from wastewater streams, and the costs associated with nutrient and water supplies for algae growth will be greatly reduced or eliminated. If it is grown in wastewater like palm oil mill effluent (POME) and can produce higher amount of lipid, which has higher application as energy raw materials. The macrophytes are considered as one type of algae species that are present in aquatic environment and have the ability to remove inorganic nutrients, toxic metals, and organic constituents. It is also widely accepted that the use of macrophytes (or weeds) in wastewater treatment is a cost effective and environment-friendly approach. Such type of species has received considerable interest as a potential feedstock and depending on the species and cultivation conditions; they can produce useful quantities of polysaccharides (sugars) and triglycerides (fats). Water hyacinth (*Eichhornia crassipes*), another type of algal species is also widely accepted in wastewater treatment as cost effective and environment-friendly approach to serve as bio-fertilizer and has potential role as carbon dioxide sink. The emission of greenhouse gases from industries such as the palm oil mill industry contribute to nearly 72% of the totally emitted greenhouse gases to be as carbon dioxide (CO_2), 18% Methane and 9% Nitrous oxide (NOx) and therefore are considered as one of the most important causes of global warming. The CO_2 is also inevitably created by burning fuels like e.g. oil, natural gas, diesel, organic-diesel, petrol, organic-petrol, and ethanol. The good news is that researchers have found the way of estimating the by product management as a measure of carbon sequestration for determining the carbon uptake and storage, which aid in restoring the security of feed stock and to serve as continuous supply for eco-balancing the cycle of providing materials and obtaining the ratio of by-product.

Theory and scientific basic to the project

The world seems to be raising its energy needs owing to an expanding population and people desire for higher living standards. Diversification bio fuel sources have become an important energy issue in recent times. Among the various resources, algal biomass had received much attention in the recent years due to its relatively high growth rate, its vast potential to reduce greenhouse gas (GHG) emissions and climate change, and their ability to store high amounts of lipids and carbohydrates. These versatile organisms can also be used for the production of bio fuel. Water hyacinth is low in lignin content (10%), high amount of cellulose (25%) and hemicellulose (35%), these show the promises of converting fermentable sugar into bioethanol which can be achieved during fermentation process and distillation mechanisms. Furthermore, in providing partial substitution of fossil fuels, biomass combustion has the potential to be carbon dioxide (CO_2) neutral compared to the burning of fossil fuels alone will contribute towards the "greenhouse" effect. This project aims to explore the opportunities for energy and bio-conversion products, encompassing micro and macro algae as good alternative sustainable waste management practice. For a quick understanding, about 1.8 tons of CO_2 are removed from the atmosphere for each ton of dry algae biomass produced. Furthermore, algae crops do not compete with human food crops, and can be grown year-round under the right conditions.

Enhancement of Biogas Productivity through Bio-pretreatment of Crop residue during Anaerobic Digestion

○Feng HONG, Fei HUANG, Chuqiao WANG, Xianning LI

School of Energy and Environment, Southeast University, Nanjing, 210096, PR China *E-mail: hong4796@seu.edu.cn

Abstract

The rice straw bio-pretreatment of aerobic composting with fermented liquor was investigated in order to increase biogas productivity in mesophilic anaerobic digestion. The biological hydrolysis effect was verified by experimental result that the lignin removal efficiency and biogas productivity increased 30.2% and 33.8% respectively in aerobic composting with raw fermented liquor, comparing to the sterilized fermented liquor. Four pretreatment factors (temperature, moisture content, size, time) were selected to evaluate its influence on hydrolysis and biogas productivity. The results indicated that the optimum operational conditions were 40℃ of temperature, 70% of moisture content, 5-10mm of size, and 3d of time, the biogas productivity could reach to 262 N-ml/g-$TS_{,substrate}$ which was 52.2% higher than that of un-pretreated crop residue.

Keywords: aerobic composting, rice straw, fermented liquor, BMP test, biogas productivity

1. Introduction

In China, the amount of crop residue generated was estimated at 650 million ton per year, comprising about 16.0% of total MSW. The crop residue belong to lingo-cellulosic substrate comprising cellulose, hemi-celluloses, and lignin. The crop residue was usually disposed by uncontrolled incineration in many farmlands for rapid minimizing and collection of potash fertilizer. This frequently caused air pollution of PM2.5, traffic accident and forest fire.

Village-scale energy center that converting crop residue to biogas has several advantages, such as low cost of feedstock collection and storage, local utilization of generated energy and process residue. Anaerobic digestion (AD) of crop residue has attracting attention for this energy center, owing to security of operation, low demand for labor, local utilization of fermented residue as fertilizer.

The biogas production efficiency is only about 20-30% with CODcr base in traditional mesophilic AD, which is largely lower than that of food waste and livestock. Generally, hydrolysis is the rate-limiting step in AD of crop residue, due to its lingo-cellulosic complex structure, which inhibits biodegradability and biogas productivity of substrate. The bio-pretreatment of aerobic composting is one of pretreatment that could promote the dissociation of lingo-cellulosic complex structure and promote biogas productivity in AD.

The aim of this study is to investigate the effect of aerobic composting on biogas productivity of crop residue in AD, to determine the optimum operational conditions such as temperature, moisture contents, size and time.

2. Materials and Methods

2.1. Substrate and inoculums

The air-dried rice straw with moisture contents of 8-9% was used as substrate, its TS content is 91%, including 86.7% of VS.

Inoculums used in this study was AD fermented liquor, which was collected from 5-L mesophilic AD reactor of rice straw. The MLVSS content concentration of fermented liquor was 20,000mg/L.

2.2 Aerobic composting pretreatment

The aerobic composting pretreatment was performed in duplicates, 60g rice straw and 53g inoculums were mixed in 1-L grass beaker. The moisture contents of inoculated substrate was about 50%, and then tap water was added to adjust moisture content of 60%, 70%, 80%, 90% respectively for different test Runs. The glass beakers were covered with plastic film which was cut several holes for aerobic condition, and then were placed in thermostat with temperature of 20℃, 30℃, 35℃, 40℃, 45℃for different test Runs. The substrate were taken out and mixed for aerobic condition every 8 hours among the pretreating period.

2.3 BMP test

Mesophilic (37 ℃) BMP tests were performed to investigate the pretreated rice straw biogas yield. The 5g-TS of pretreated substrates were added with 200ml inoculum in a 250-ml glass bottle. Each bottle was flushed with N2 for 2min to replace the oxygen gas, and then covered with rubber stopper, placed in shaking water bath at 37℃ with 130rpm. During the BMP test period, the biogas volume was measured using water replacement method.

3. Results and Discussion

3.1. The effect of biological hydrolysis during pretreatment

The rice straw pretreatment of aerobic composting was performed by three Runs, raw fermented liquor used as inoculum in Run 1, sterilized fermented liquor used as

inoculum in Run 2. The Run 3 was the blanket test without pretreating, only performed in BMP test. As shown in **Fig.1**, the removal efficiency of cellulose, hemi-cellulose, lignin after pretreatment in Run 1 was higher than that of Run 2, the lignin removal efficiency increased 30.2% with comparison of R1 and Run2.

The daily biogas yield of Run1 had been always greater than that of Run 2 and 3, the cumulative biogas yield after 24 days in Run 1 reached to 239.4 N-ml/g-TS,$_{substrate}$, which was 33.8% higher than that of Run 2.

After 3days aerobic composting in Run 1, white hairy materials appeared in the substrate, was thought as fungus. According to above test result, the biological hydrolysis effect of aerobic composting was confirmed.

3.2. The optimum pretreatment conditions

The operational factors (temperature, moisture, size, time) of aerobic composting were selected to investigate its influence on performance of pretreatment by the index of organic content (cellulose, hemi-cellulose, lignin) removal efficiency after pretreatment and biogas productivity in mesophilic BMP test. Fig.2 showed the test result of 4 operational factors (temperature, moisture, size, time) from upper to bottom about organic content removal efficiency and biogas productivity.

The lignin removal efficiency increase with temperature increasing, cellulose and hemi-cellulose removal efficiency was lowest under condition of 40℃. The biogas yield and producing constant was highest under condition of 40℃, 245N-ml/g-TS,substrate and 0.0434d-1 respectively.

The cellulose removal efficiency of 70% and 80% moisture test were significantly lower than that of other tests, was about 4.0-8.0%. The biogas yield under moisture contents condition of 70-80% was higher than that of other tests, 245-248N-ml/g-TS,substrate.

About the influence of chopped size, the removal efficiency of cellulose, hemi-cellulose, lignin was nearly same, the biogas yield increased with chopped size, about in the range of 245-262 N-ml/g-TS,substrate.

The removal efficiency of cellulose, hemi-cellulose, lignin increased with the prolonging of pretreatment time. At the pretreatment condition of 2 days, the biogas yield reached to top value, was about 245 N-ml/g-TS,substrate.

The above results indicated that the optimum operational conditions were 40℃ of temperature, 70% of moisture content, 5-10mm of size, and 3d of time.

4. Conclusions

(1) The biogas yield of rice straw could be improved after pretreatment of aerobic composting.

(2) The biological hydrolysis effect of aerobic composting was confirmed by the addition of raw fermented liquor.

(3) The optimum operational conditions of aerobic composting were 40℃ of temperature, 70% of moisture content, 5-10mm of size, and 3d of time.

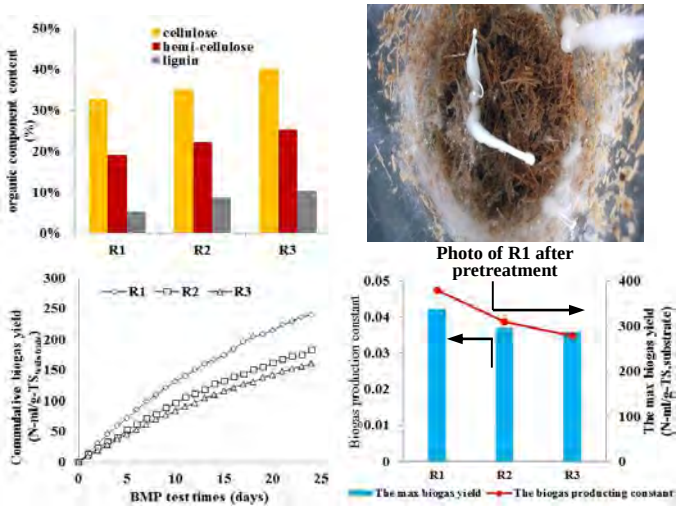

R1: Pretreatment of raw fermented liquor as inoculum
R2: Pretreatment of sterilized fermented liquor as inoculum
R3: Un-pretreatment

Fig.1. Performance of pretreatment of aerobic composting

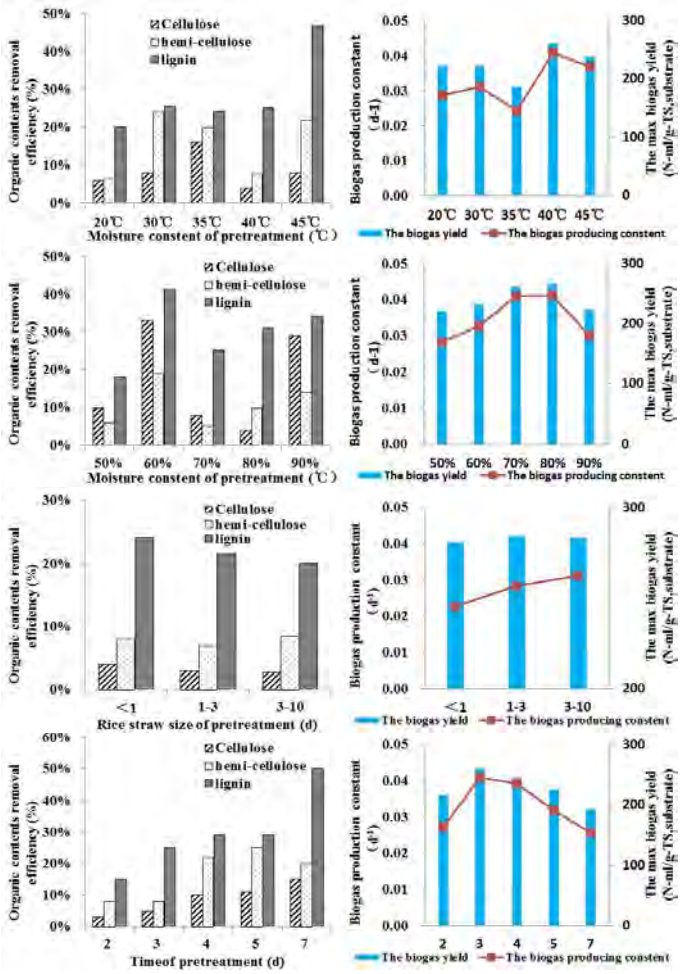

Fig.2. The influence of operational factors on organic materials removal efficiency and biogas productivity in BMP test

Geomorphological recession flow model for estimation of drainable storage

Basudev Biswal[1,*], Marco Marani[2] and D. Nagesh Kumar[3]
[1]Department of Civil Engineering, Indian Institute of Technology Hyderabad, Hyderabad, India
[2]Department of Civil and Environmental Engineering, Duke University, Durham, USA
[3]Department of Civil Engineering, Indian Institute of Science, Bangalore, India
*Email: basudev@iith.ac.in

Abstract

The hydrologic response of watersheds is a result of the interplay between three dominant controls: climate, landscape and vegetation. The response of a basin to rainfall events has been shown to be linked to the basic structural organizations of its channel networks. This has led to development of hydrologic response model based on channel network morphology for various practical applications. This talk will particularly discuss about geomorphological recession flow model and the issue of 'drainable' storage estimation. Drainable storage can easily be computed for a rainfall-runoff event by taking the area under the 'complete' recession flow curve (i.e. a discharge vs. time curve where discharge continuously decreases till it approaches zero). But a major challenge in this regard is that recession curves are rarely 'complete' due to short inter-storm time intervals. Therefore, it is essential to analyze and model recession flows meaningfully. Here Brutsaert and Nieber method is adopted for recession analysis which expresses time derivative of discharge *dQ*/*dt* as a power law function of Q: $-dQ/dt = kQ^{\alpha}$. However, the problem with *dQ*/*dt*-*Q* analysis is that it is not suitable for late recession flows. Traditional studies often compute α considering early recession flows and assume that its value is constant for the whole recession event. But this approach gives unrealistic results when $\alpha \geq 2$, a common case. The issue is addressed here by using geomorphological recession flow model that exploits the dynamics of active drainage networks. According to the model, α is close to 2 for early recession flows and 0 for late recession flows. A simple expression for drainable storage is then derived, which is a function of k and basin area. Using 121 complete recession curves from 27 USGS basins it is showed that predicted drainable storage matches well with observed drainable storage, indicating that the model can also reliably estimate drainable storage for 'incomplete' recession events to address many challenges related to water resources.

1. Introduction

River networks exhibit remarkable morphological and structural similarities, which can be expressed quantitatively through traditional and fractal geometry. One important question thereupon is how the spatial organization of river networks is reflected in the hydrologic response to rainfall inputs. Several studies in the past have discussed about the relationship between basin geomorphology and hydrologic response, particularly during flood periods. Here we particularly discuss about how basin geomorphology controls recession or drought flows.

1.1. Recession flow analysis and modelling

A systematic recession flow analysis arguably began with the work by Brutsaert and Nieber, who expressed dQ/dt as a function of Q (Q being discharge at the basin outlet at time t). They found that dQ/dt typically exhibits a power law relationship with Q during recession periods: $-dQ/dt = kQ^{\alpha}$. In generally practice the parameters α and k for a basin are obtained by considering (dQ/dt, Q) data points from all recession events together. However, recent studies show that dQ/dt-Q curves from different events are very different from one another (quantified in terms of k), meaning that recession flow curves need to be analyzed individually. Recent studies have shown that recession flow curve properties of a basin can be modelled by considering its channel network morphology.

At any point of time, Q can be expressed as a product of flow generation per unit length (q) and total length of the channel network contributing flow $G(t)$: $Q = q \cdot G(t)$. If we assume that q and the rate at which the channel network shrinks in downstream direction (c) are constant, we will find that $-dQ/dt = qc \cdot N(t)$. That means $N(l) = \rho G(l)^{\alpha}$, where $l = c \cdot t$ and $\rho = kq^{\alpha-1}/c$. It is generally found that the value of α obtained by considering channel network is quite close to that of obtained by considering real recession curves. That means we can model recession flows by considering the geomorphological recession flow model for various practical purposes. In the next section we will discuss about how the geomorphological recession flow model for model can be used to estimate drainable storage.

2. Estimation of drainable storage

Storage of water within a river basin is often estimated by analyzing recession flow curves as it cannot be instantly estimated with the aid of available technologies. For example, GRACE (Gravity Recovery and Climate Experiment) satellites can measure storage fluctuation, but cannot measure absolute storage. In this study, we particularly discuss about drainable storage (SD) or the part of basin storage that turns into streams flows. If a recession event is sufficiently long such that discharge approaches zero in the end (i.e. the recession event is 'complete'), drainable storage can be computed simply by integrating discharge over time. However, in most real scenarios recession events are 'incomplete.' Therefore, a recession flow model must be used to construct a pseudo-complete recession curve to compute drainable storage. In earlier times it was assumed that the value of α for a basin is constant throughout a recession event. However, this assumption would suggest that drainable storage is infinite when $\alpha \geq 2$, which is a common case. That means α cannot remain constant throughout a recession event. The geomorphological recession flow model suggests that for natural basins in general α is 2 for early recession flows and 0 for late recession flows. Therefore, it can be seen that drainable storage-discharge curves exhibit two distinct relationships distinguished from one another by a sharp transition. This behavior is very well captured by the geomorphological recession flow model. After following suitable mathematical procedures a simple mathematical equation for initial drainable storage (drainable storage at the beginning of a recession event) is obtained: $SD_0 = 0.5/k \cdot [1 + \ln(A)]$, where A is basin area. It should be noted that k can be computed using a few days of recession flow data only. Finally, the model's performance is evaluated done by considering 121 complete recession events, for which the values of k were obtained by considering early recession flows only. It was found that modelled drainable storage matches well with observed drainable storage ($R^2 = 0.96$, see Fig. 1).

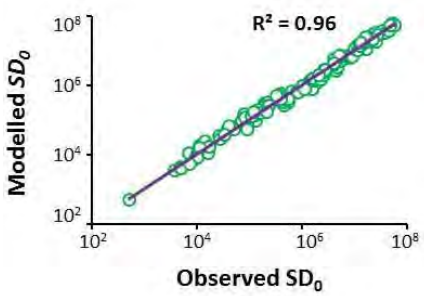

Fig. 1. Modelled drainable storage vs. observed drainable storage.

3. Conclusions

Recession flows can be modelled by considering the morphology of channel networks. The geomorphological recession flow model predicts the value of exponent α quite well. It is also found that the model very well mimics the scaling transition in drainable storage-discharge curves. Finally, the ability of the model in estimating drainable storage indicates that it can be used to compute drainable storage for incomplete recession events to solve many practical problems related to water resources management.

Session III

Presentations by students

Preparation and evaluation of fermentation liquid of food waste as a carbon source for denitrification

○Yongmei ZHANG[1], Xiaochang WANG[1*], Zhe CHENG[1], Yu-You LI[2], Jialing TANG[1]

[1] Key Lab of Northwest Water Resource, Environment and Ecology, MOE, Xi'an University of Architecture and Technology, Xi'an 710055, P.R. China

[2] Graduate School of Environmental Studies, Tohoku University, 6-6-06 Aza-Aoba, Aramaki, Aoba-ku, Sendai, Miyagi 980-8579, Japan

*E-mail: xcwang@xauat.edu.cn

Abstract

The anaerobic fermentation of food waste with different temperature and initial substrate concentration were studied when considering total amount of organic acids production, and then the carbonaceous mixture was evaluated as an alternative carbon source for denitrification performance using batch nitrate utilization rate tests (NURs) under different initial COD/N ratios. The denitrification kinetics parameters depended on initial COD/N ratios such that the maximum rate value of 14.11mgN/gVSS·h with COD/N ratio of 10, however, the maximum potential value of 0.299gN/gCOD with COD/N ratio of 2. The obvious linear relationships between values of nitrogen reduction and COD consumption were obtained, and the maximum readily biodegradable fraction in FLFW was obtained for ratio of 6.

Keywords: Food waste, anaerobic fermentation, carbon source, denitrification performance, COD/N ratio

1. Introduction

The process of anaerobic digestion consists of four steps: hydrolysis, acidogensis, acetogenesis and methanogenesis, and the fermentation production in the first two steps is viable alternative carbon source for denitrification process due to the effluent rich in dissolved organic matter composed of organic acids, primarily acetate, propionic and lactic acid. The temperature and initial substrate concentration affect the amount and types of each fermentation production, and selecting a suitable operation condition is also crucial to enhance organic acids production. The optimum organic acids production were studied in previous reports, however, there were few reasearchs on the denitrification effects of these complex mixture as an alternative carbon source.

In this study, firstly selection of optimum conditions of anaerobic fermentation was determined and then the denitrification characteristic of fermentation liquid (FLFW) was evaluated with nitrate utilzation tests (NURs) as an alternative carbon source.

2. Materials and Methods

2.1 Fermentation material and inoculums

The fermentation material was taken from a student restaurant. In each collection, bones and insert material (paper and plastic) were discarded, only the fermentable material was preserved. After selecting the waste, it was firstly heated treatment through enough boiled water with the aim of greatly avoiding the inhibition from waste oil, and then was crushed and homogenized in a blender to ensure the particle size less than 5mm.

Anaerobic activated sludge from Xi'an Siyuan wastewater treatment, whose operation mode is anaerobic-anoxia-aerobic activated sludge reactor and continuously run for 2 years, was used as the inoculums, after natural sedimentation for one day.

2.2 Experimental procedures

The anaerobic digestion experiments were conducted in a single-stage reactor with a working volume of 10L. The operation conditions were shown in Table 1.

Table 1 Operation conditions for Run1-Run6

Parameters	R1	R2	R3	R4	R5	R6
Temperature	35℃	55℃	25℃	25℃	25℃	25℃
Substrate concentration	11%	11%	11%	9%	13%	15%

The sealed conical flask reactors (1L) were used in the batch experiments to investigate the effects of COD/N ratios on denitrification performance when using FLFW as carbon source. Various quantities FLWF and NaNO3 solutions were added into the reactors with synthetic wastewater, giving the initial COD/ NO3-N of 2, 4, 6, 8 and 10, respectively. All the reactors were placed on stirring plates in constant temperature incubator at 25±1℃. The initial pH values in all batch experiments were adjusted to 7.5±0.2 using 0.5M NaOH and 0.5M HCl solution.

3. Results and Discussion

3.1. Selection of optimum fermentation condition

Fig.1 shows that carbohydrate degradation was extreme due to operation conditions, but the protein degradation was generally reached at 20±2% except for when temperature was at 55 ℃ .Apparently, the carbohydrate and protein degradation at high temperature were significantly lower than other conditions, which were because that higher temperature inhibited activity of

acidification bacterial. The obvious negative relationship between initial substrate concentration and removal efficiencies of carbohydrate was found in this study.

Hydrolysis phase during solid wastes degradation can be considered as limiting step because wastes are often particulate material. The hydrolysis rate seems to be only related with temperature, and a higher hydrolysis and a lower acidogenesis of food waste at a higher temperature were observed. Acetate and lactic acid are prevalent organic acids under all conditions. Taken together, basing on the views of acidogenesis rate and total organic acids amounts, the fermentation liquid at optimum condition R5 (25℃ and 13% of substrate concentration) was selected as alternative carbon source to evaluate its denitrification performance.

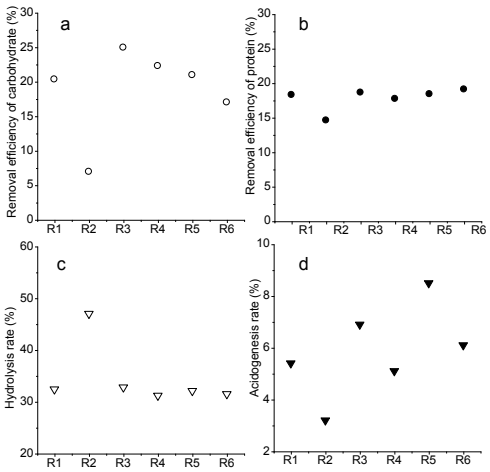

Fig.1 Effect of operation conditions on fermentation parameters.

3.2. Evaluation denitrification performance of FLFW as carbon source

Fig.2 illustrates the transformation of NO_3-N, NO_2-N and COD in denitrification process using FLFW as carbon and electron sources under different COD/N ratios. Incomplete denitrification process occurs when carbon is limiting and is characterized by large fractions of residual nitrate and slight nitrite accumulation at the end of the process when COD/N ratios were 2 and 4. At ratios up to 6 and 8, complete denitrification (nitrogen in effluent less than 1mg/L) were obtained, which indicated that denitrification was limited by carbon amount rather than carbon availability. With respect to residual COD in the effluent, values lower than 30mg/L with ratios of 2, 4 and 6, while increased concentration with ratios of 8 and 10 were obtained in the treated effluent after 4.5h reaction. In view of results obtained, so the optimum COD/N ratio (where both COD and N concentrations reached minimum in the effluent) for FLFW is 6.

Three linear phases of NOx-N reduction occur simultaneously during the process of denitrification (Fig.3). The maximum denitrification rates are obtained in the first 80 or 100 minutes of reaction, with values ranging between 11.65 and 14.11mg/gVSS·h, depending on the COD/N ratio employed. The denitrification potential ranged between 0.133 and 0.299gN/gCOD. There was a negative relationship between p_{DN} and COD/N ratio, where the greatest p_{DN} was more than twice of the lowest value.

The readily biodegradable fractions (S_S) were calculated by p_{DN}, and the slowly biodegradable fraction (X_S) was calculated from the measured SS and the known total COD added. And the maximum fraction of S_S was 58.35% with COD/N ratio of 6.

4. Conclusions

(1) Temperature (25℃) and substrate concentration (13%) were selected as optimum operation condition for anaerobic fermentation of food wastes.

(2)The optimum COD/N ratio was 6 for free values of COD and nitrogen in effluent when batch NURs were performed.

(3)The maximum denitrification rate and maximum denitrification potential reached with ratios of 10 and 2, respectively.

(4) The readily biodegradable fraction of FLFW was 58.35%.

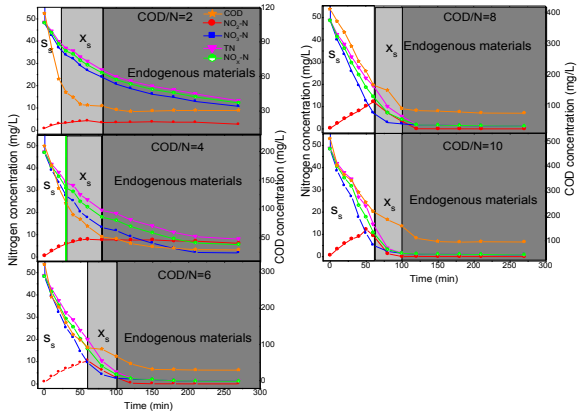

Fig.2 Variation of TN, NO_2^--N, NO_3^--N, NO_X^--N and COD with the electron donor of FLFW.

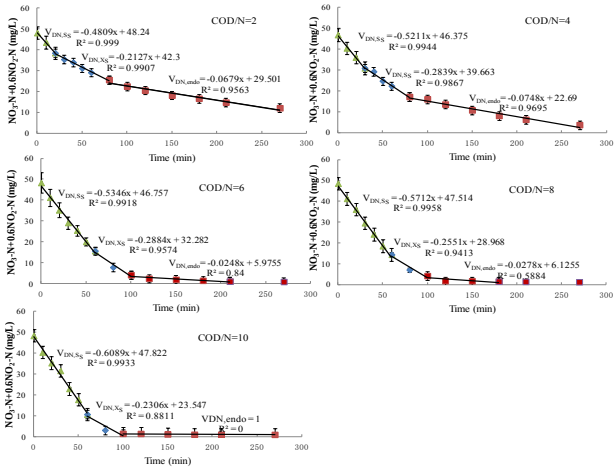

Fig.3 NO_X-N profiles for different COD/N ratios when using FLFW as carbon source.

Nitrogen removal enhancement in A/O-MBR with fermentation liquid of food waste (FLFW) as external carbon

Jialing Tang, Xiaochang Wang*

(School of Environmental and Municipal Engineering, Xi'an University of Architecture and Technology, Xi'an 710055, China)
**E-mail: tangjialing88@126.com*

Abstract

Fermentation liquid of food waste (FLFW) was applied as external carbon to enhance N removal in A/O-MBR. Results showed that FLFW characterizes high denitrification potential and can be regarded as readily degradable carbon. The denitrification was enhanced after adding FLFW in pilot A/O-MBR, and high N removal was achieved (above 65%). Moreover, FLFW did not cause serious membrane fouling, and the fouling can be effectively controlled by chemical clean.

Keywords: Fermentation liquid of food waste (FLFW), A/O-MBR, nitrogen removal, membrane fouling

1. Introduction

Nutrient pollution caused by excess nitrogen and phosphate discharge has been hotly discussed and studied in recent years. The commonly applied nitrogen removal pathway was achieved through nitrification and denitrification to reduce ammonia into nitrogen gas with organic matter as electron donor. Low organic matters in wastewater always restrict nitrogen removal for low energy for substrate transport and biomass produce. So in practice, external carbon was always added to increase the C/N in influent and enhance nitrogen removal. Glucose or acetate was used for wastewater treatment, but the cost was too high for full-scale plants. In this background, to find economic and environment-friendly external carbon is always the object for researchers.

Food wastes contain high organic matters and are easily degradable which was suitable to be chosen as external carbon source. So in this study, food waste fermentation liquid was added into A/O-MBR as external carbon to improve nitrogen removal. Nitrogen removal characters and membrane fouling were the main concerns in this study.

2. Materials and Methods

2.1. A/O-MBR

A lab and pilot-scale A/O-MBR were involved to study the characters and nitrogen removal efficiencies in this research. The lab-scale one was 37.5L, while the pilot one was 8m^3. MLSS and in two reactors were both 3000-4000mg/L. HRT in lab one was 17h and in pilot one was 8h. The membrane surface area was 0.5m^2 and 10m^2 respectively. Pore sizes of the hollow fiber membrane were 0.2μm. Recycle rate of the two MBR were both 2. Glucose, Sodium Acetate and FLFW were applied as carbon sources in lab-scale A/O-MBR. COD and TN in influent were 300-350mg/L and 25-35mg/L.

2.2 Analysis methods

The N compounds and COD were measured every day according to APHA. The TMP was recorded by on-line meters. Membrane fibers were cut from the membrane frame before and after the chemical clean to survey the effect of chemical clean on membrane fouling control. AFM was applied to observe the surface of membrane. EEM of the Dissolved Organic Matters (DOM) in influent, supernatant and effluent were got to analyze the membrane fouling. EPS were extracted and analyzed to explain the membrane fouling.

3. Results and Discussion

3.1. Denitrification potential of FLFW

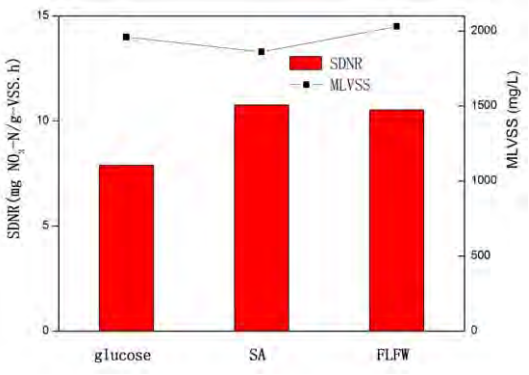

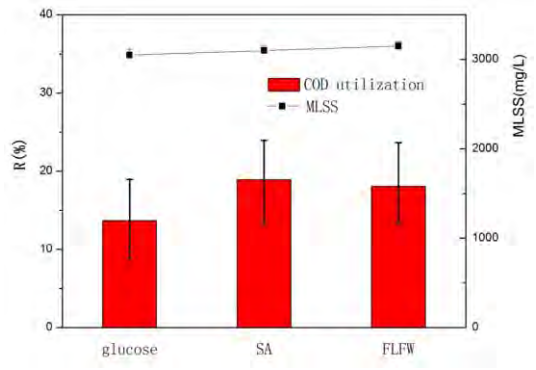

Fig. 1 Denitrification rate and COD utilization rate of FLFW

The specific denitrification rates (SDNR) of the three external carbons were shown in figure 1. It can be seen that the SDNR of FLFW was very close to Sodium Acetate (SA), but higher than that of glucose. The results demonstrated that the FLFW characterizes high denitrification capacity and could be regarded as readily degradable carbon source. The COD utilization efficiency of these three carbon sources were the same to that of SDNR, which also meant that the FLFW owns the high denitrification potential.

3.2. N removal in pilot MBR

It can be seen in figure 2 that after adding FLFW, the denitrification was enhanced and the TN in effluent decreased sharply. The TN removal efficiencies increased from 30% to 65%. In addition, the higher the COD was in influent, the lower the TN was in effluent. And the TN removal also was influenced by HRT. The longer HRT caused the higher TN removal.

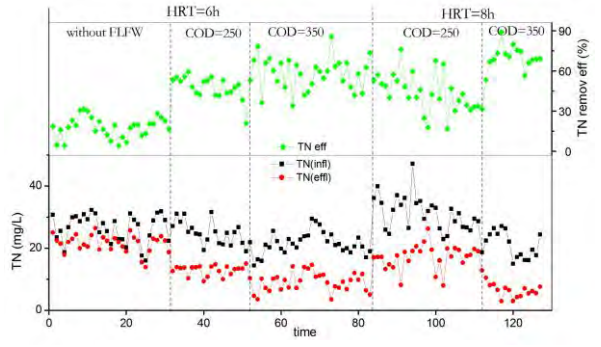

Fig. 2 TN removal in pilot A/O-MBR

3.3. Membrane fouling

It can be seen in figure 3, the TMP increased slowly before and after FLFW addition, which demonstrated that the FLFW did not cause serious membrane fouling in our operation conditions. The fouling rate (FR) was a little higher after adding FLFW (from 158Pa/d to 198Pa/d), and the longer HRT can slow down the FR. Chemical clean can effectively decrease membrane fouling.

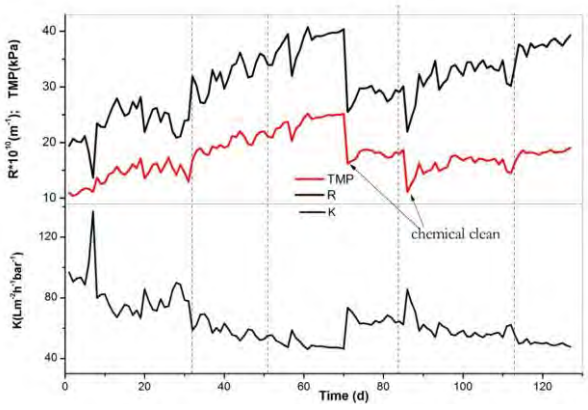

Fig. 3 Variation of TMP, Resistance of pilot A/O-MBR

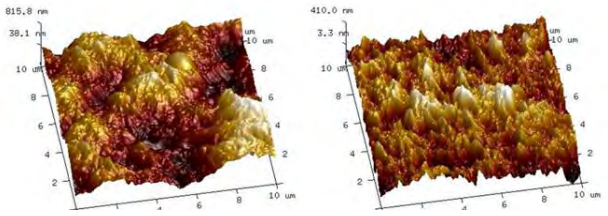

Fig. 4 AFM images of membrane before and after chemical clean

From figure 4, it can be seen that the surface of membrane before and after chemical clean. It can be seen that the pores on the surface was blocked by sludge or other compounds, while after chemical clean, the pores could be seen clearly. That is why the TMP decreased sharply after chemical clean. But some pores were still fouled, which was the reason why the resistance (R) cannot decrease to the former stage (figure 3).

4. Conclusions

5. FLFW was utilized as external carbon to enhance N removal in A/O-MBR. The results demonstrated that, same to sodium acetate, the FLFW characterizes high denitrification potential and COD utilization, can be regarded as readily degradable carbon source. And the pilot MBR achieved high N removal after adding FLFW. The membrane fouling increased slightly, but can be effectively controlled by chemical clean.

Structure Optimization of Constructed Wetland Coupled Microbial Fuel Cell for Organism Removal

○Xizi LONG[1]*, Xianning LI[1], Hailiang SONG[1], Feng HONG[1] , Wenli XIANG[1]
[1]School of Energy and Environment, Southeast University, Nanjing 210096, China
*E-mail: 230149343@seu.edu.cn

Abstract
Constructed wetland was employed to generate electricity due to the different potentials between aerobic zone (high position) and anaerobic zone (low position). The experiment for optimizing the condition used current (density), power density and internal resistance as parameters to characterize the performance of electricity generation. Resulting from changing the spacing between the anode and cathode, 20cm spacing exhibited the best performance (94.9% COD removal rate, 0.149W/m^3 Power density, 339.8Ω internal resistance). In brief, the optimal operation contributed to achieving practical implementation.

Keywords: constructed wetland, microbial fuel cell, spacing, structure optimization

1. Introduction
Microbial fuel cells (MFCs) function as a promising new energy technology for electricity generation in parallel to acquire benefits for the environment, which make use of domestic sewage, effluent of industry, leachate, sediment and rhizodeposits as biodegradable substrates. A large number of investigations have been devoted to exploit the MFCs construction in nature successfully, thus a difference of potential between the anode (positive) and the cathode (negative).

Apparently, constructed wetland owns places with different redox potential either conversing organic matters to electrons by exoelectrogens or acting as cathode with high level of dissolved oxygen, which indicates the feasibility to assemble constructed wetland into some kinds of MFC and has been improved to enhance the degradation of dye in wastewater in some cases.

This work aimed to explore the structure of constructed wetland coupled microbial fuel cell (CWMFC) to obtain the optimized the space between two electrodes.

2. Materials and Methods
2.1. Constructed wetland coupled microbial fuel cell fabrication
CWMFC was integrated with a vertical organic glass pipe, as shown in Fig.1. Both of two electrodes consisted of granular activated carbon. Stainless steel mesh current collector buried in the electrode was linked with insulated titanium wire to external circuit which connected to potentiostat. The total volume of the installation was 35.3L with total efficient volume of 12.4L compared to anode of 7L and 2.1L of efficient volume. To culture microorganisms, condensed anaerobic slurry (20g/L mixed liquid suspended solids) was added into CWMFC and the synthetic wastewater was transported by a peristaltic pump. The hydraulic retention time was reckoned 48h and the installation had a flow of 6.36 mL/min.The components of wastewater are as follows:

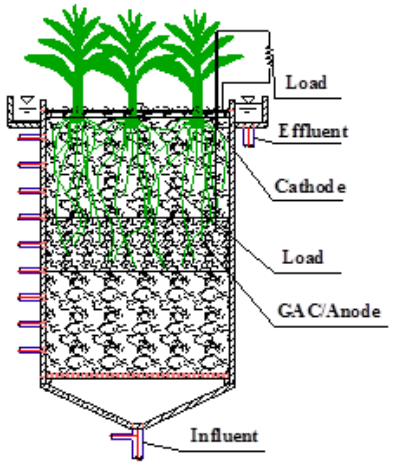

Fig. 1 Experiment installation

Glucose 200mg/L, KNO_3 252.5mg/L, $K_2HPO_4 \cdot 3H_2O$ 26.32mg/L, $NaHCO_3$ 336mg/L, NaCl 330mg/L and 10 mL micronutrients.

2.2 Experimental procedures
The anode located in10cm, 20cm, 30cm and 40cm position far from the cathode (Fig.2) respectively to explore the factors of different distances between the two electrodes.

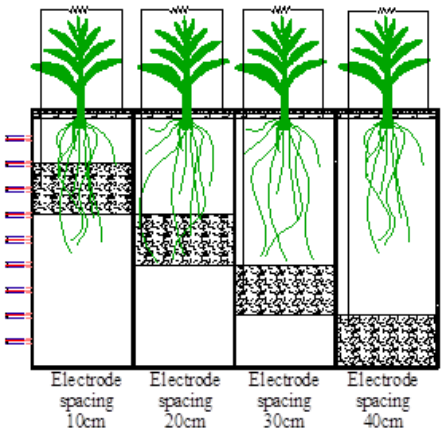

Fig. 2 CWMFCs with difference electrode spacing

3. Results and Discussion

The evolution of voltages of different spacing between two electrodes during the experiment was shown (Fig.3).The voltages of 20cm were recorded in the order of 560mV throughout the experiment, while 30cm resulted in 520mV. However, the 10cm, 40cm just approximately reached 440mV, 420mV respectively.

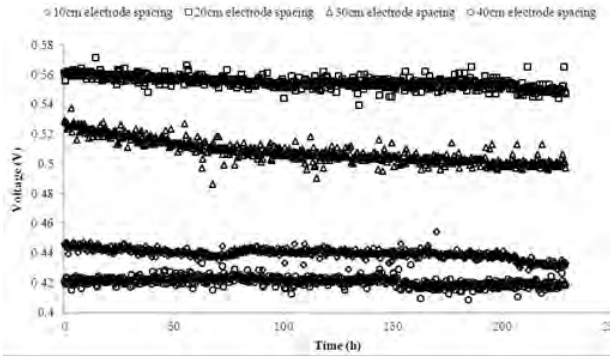

Fig. 3 The evolution of voltages of difference electrode spacing

Fig.4 portrayed polarization profiles and power density profiles. The maximum open circuit voltage, 741mV, was achieved at 20cm spacing which obtained the maximum current density of 0.486A/m^{3}and the maximum power density of 0.198 W/m^3 with about 400 Ω external resistance. The internal resistance(R_{int}) was reckoned to be 385.8 Ω (R_{int},10cm),339.8 Ω(R_{int},20cm), 367.68Ω(R_{int},30cm) and 406.32 Ω(R_{int},40cm) by linear part of polarization curves(the external resistance varied between 100−1000Ω).

When feeding on the same synthetic wastewater, the cathode potential was determined primarily by the dissolved oxygen, after all, the reactions occurring in the MFC determined the electrodes potential. On the contrary, the anaerobic condition conformed to the exoelectrogens as the efficient catalyst which suggested that the electricity producing was closely related to the level of DO.

The COD removal efficiency of 4 kinds of electrode spacing against reactor height was shown in Fig.5 with 1000Ω external resistance at continuous flow. The 20cm

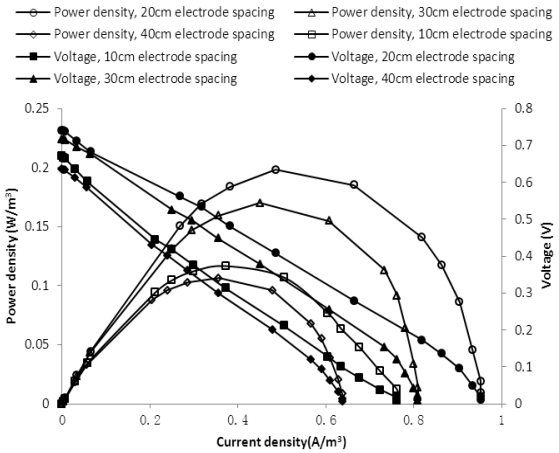

Fig. 4 The polarization curves and the power density-current density curves

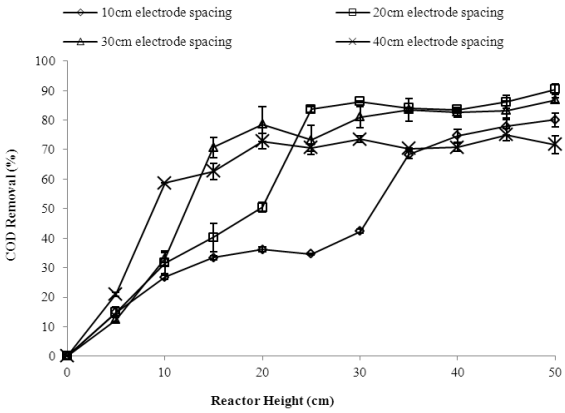

Fig. 5 COD removal efficiency of 4 kinds of electrode spacing

spacing achieved the minimum effluent COD concentration of 11mg/L, thus the maximum COD removal efficiency of 94% and features of electricity (power density 0.149 W/m^3, coulombic efficiency 0.313%). According to the curves, a huge drop of COD concentration exactly in each anode compartment was observed which demonstrated the excellent oxidation efficiency of the anode based on the granular activated carbon anode material with huge specific surface area for biomass adsorption. MFC with higher current generation also facilitated the terminal COD removal.

4. Conclusion

In this constructed wetland coupled microbial fuel Cell system, optimal spacing (20cm) between two electrodes can enhance the process of electricity generation and organism removal.

Analysis of enhanced nitrogen removal in MBR with new biological carriers addition by real-time PCR

○Yuli YANG[1], Hailiang SONG[2], Xiaoli YANG[1]*

[1]School of Civil Engineering, Southeast University, Nanjing, 210096, PR China
[2]School of Energy and Environment, Southeast University, Nanjing, 210096, PR China
*E-mail: yangxiaoli@seu.edu.cn

Abstract

The effect of new biological carriers' addition on nitrogen removal and denitrifying microbial flora and functional enzymes by real-time PCR were investigated in six submerged membrane bioreactor. The mean density of AOB, NOB, amoA, nirS gene obtained by real-time PCR was 10^6/mL, 10^8/mL, 10^5/mL and 10^{19}/mL, respectively. Carbon source and DO had a great effect on TN removal. The mean TN removal rate in MBR with modified carriers addition reached to 40.69%, which was higher than the control MBR (13.72%). Modified biological carriers were proved to be effective in enhancing nitrogen removal with easy operation.

Key words: MBR; biological carrier; real-time PCR; enhanced nitrogen removal; microbial flora; functional enzyme

1. Introduction

One of the major drawbacks of MBR was lack of carbon sources and insufficiency of total nitrogen removal. It was necessary that a new MBR should be introduced to enhance nitrogen removal. A new submerged hybrid biological carrier MBR was constructed to enhance nitrogen removal by adding a certain amount of agricultural wastes. As nitrification and denitrification were biological processes, understanding the ecology of microorganisms involved may ultimately lead to the improvement of nitrogen removal. Real-time PCR was helpful to solve environmental engineering problem as a powerful approach and had allowed studies of bacterial community populations in response to varying environmental conditions. This constitutes significant progress for microbial ecology studies as it had been estimated that only a minor proportion (about 1%) of naturally occurring microorganisms have been isolated in pure culture experiments.

This study investigated the effect of DO concentration, the carrier types and the carbon source properties on the removal of nitrogen in MBR. Comparative research was conducted in order to reveal the mechanism of enhanced nitrogen removal with new type of biological carriers' addition. And real-time PCR was used to reveal the changes of these microbial floras and functional enzymes.

2. Materials and Methods

2.1. Experimental facilities

There were six parallel operation MBRs in this experiment, which were cylindrical with the dischargeable capacity of 10L. The operation conditions of different MBR were shown in Table 1.

Synthetic wastewater was adopted in this experiment. COD, NH_4^+-N, TP of influent water was controlled at 200mg/L, 40mg/L and 5mg/L, respectively. The modified of biological carriers was to soak them in 2% Sodium hydroxide for 24h.

Table 1 Reactor operation parameters

Reactor	Filler and carbon source	DO (mg/L)
1#	liquid carbon source（ethanol）	3
2#	PVC carrier（polyhedral hollow sphere PVC）	3
3#	blank（no extra carbon source and carrier）	3
4#	low DO（no extra carbon source and carrier）	1.5
5#	unmodified carrier（unmodified straw）	3
6#	modified carrier（modified straw）	3

2.2 Experimental procedures

DNA isolation from the mixed sludge in MBR was performed by using Ezup® column Soil Genomic DNA exaction kit. For PCR purposes, the DNA concentration was measured spectrophotometrically. PCR amplification of 16S rRNA genes, amoA, nirS genes was performed in a total volume of 25μl in an Applied Biosystems 2720 Thermocycler. Table 2 shows PCR primers in this study.

Table 2 Primer sets included in PCR assay

Target gene	Nucleotide sequence (5′–3′)
16S rRNA AOB	GGAGRAAAGCAGGGGATCG
	GGAGGAAAGTAGGGGATCG
	CTAGCYTTGYAGTTTCAAACGC
16S rRNA NOB	CCTGCTTTCAGTTGCTACCG
	GTTTGCAGCGCTTTGTACCG
	CTAAAACTCAAAGGAATTGA
amoA	GGGGTTTCTACTGGTGGT
	CCCCTCKGSAAAGCCTTCTTC
nirS	GTSAACGTSAAGGARACSGG
	GASTTCGGRTGSGTCTTGA

The annealing temperature of AOB, NOB, amoA, nirS was 55°C, 50°C, 65°C, 57°C. Amplification of quantitative PCR products was carried out with an ABI Step One Plus by using SYBR green as the detection system. The template

copy number was determined from C_T values by using a standard curve.

3.1. Nitrogen removal

The removal of NH_4^+-N was irrespective of the operating conditions and achieved a high removal. However, TN removal rate varied a lot with the removal rate in the order of adding liquid carbon MBR > low DO condition > adding modified carriers MBR, and the order of nitrate nitrogen was just the opposite (table 3). When using carbon source of modified carrier, the amount of nitrite nitrogen was less. The TN removal rate was higher. The difficulty of carbon source utilization had great effect on nitrate nitrogen, which indicated that carbon source have great impact on denitrification. Adding modified carriers MBR not only could form micro environment, but also could provide the carbon source. So it improved nitrogen removal effectively in consideration of the economic situation.

Table 3 Nitrogen removal in the 6 reactors. All the values are given as mean (n=18).

	NH_4^+rem oval rate/%	TN removal rate/%	NO_3^- /(mg/L)
PVC	96	30	27
low DO	98.4	44.49	21.31
liquid carbon	95.01	49.48	18.33
blank	96.61	13.72	33.03
unmodified carriers	97.37	32.69	25.75
modified carriers	98.65	40.69	23.18

3.2. Quantification of 16S rRNA, amoA, nirS genes

The mean density of AOB, NOB, amoA, nirS gene in six reactor obtained by real-time PCR is 10^6/mL, 10^8/mL, 10^5/mL and 10^{19}/mL, respectively (table 4). The density of ammonia oxidizing bacteria of adding unmodified biological carriers MBR were obviously more than the other reactors, but the density of ammonia monooxygenase was the lowest. There was no correlation between ammonia oxidizing bacteria and ammonia monooxygenase, which indicated that ammonia monooxygenase activity was not only by ammonia oxidizing bacteria, but also existed other bacteria of ammonia oxidation function. Because the high removal rate of ammonia nitrogen, ammonia oxidation was not the limiting factor for nitrogen removal. The density of nitrite oxidizing bacteria of low DO condition was obviously lowest, and nitrate nitrogen was relatively low. It can be supposed that DO was in favor of nitrite oxidizing bacteria's growth and low DO could realize short-cut nitrification. The highest nitrate concentration was achieved when no carbon source was added. This proved that nitrite oxidizing bacteria was autotrophic bacteria. The density of nirS of adding liquid carbon MBR and adding modified carriers MBR was obviously highest, followed by low DO condition and adding PVC carriers MBR. Adding liquid carbon MBR and low DO condition's nitrate nitrogen rather low, which indicated that carbon source and low DO are beneficial for denitrification, which suggested that denitrification in MBR was heterotrophic anaerobic process. Denitrification in MBR with modified carriers addition was also perfect because of its abundant microorganisms and available carbon source carriers. There was a significant correlation between TN removal and density of nirS (table 5), which indicated that denitrification in MBR was the key process for nitrogen removal. Therefore, TN removal of adding modified carriers MBR was also perfect.

Table 4 The density of 16S rRNA, amoA, nirS genes (number/mL). All the values are given as mean (n=10).

	AOB	NOB	amoA	nirS
PVC	5.00E+06	3.00E+08	22505	1.00E+19
low DO	3.00E+06	2.00E+08	32522	2.00E+19
liquid carbon	7.00E+06	3.00E+08	37273	1.00E+20
blank	7.00E+06	3.00E+08	21112	9.00E+18
unmodified carriers	1.00E+07	3.00E+08	18527	8.00E+18
modified carriers	6.00E+06	3.00E+08	43073	1.00E+20

Table 5 The relationship between TN removal and nirS gens (n=10).

The reactor type	TN removal rate and nirS gens	
	r	*p*
PVC carrier	-0.948**	0
low DO	-0.837**	0.01
liquid carbon source	-0.959**	0
blank	-0.745*	0.034
unmodified carriers	-0.959**	0.057
modified carriers	-0.931**	0.001

r is the correlation coefficient; *p* is the Pearson's correlation coefficient; ** Significant correlation at the 0.05 leve; * Significant correlation at the 0.01 leve.

3. Conclusions

(1) The mean density of AOB, NOB, amoA, nirS gene in MBR obtained by real-time PCR is 10^6/mL, 10^8/mL, 10^5/mL and 10^{19}/mL, respectively.

(2) Carbon source and DO had a great effect on TN removal. Modified carriers were effective in improving nitrogen removal of MBR.

Effect of oysters on size-fractionated marine phytoplankton communities in Shizugawa bay

○Yizhe ZHENG[1], Kyohei Hayashi [2], Takashi Sakamaki [3], Osamu Nishimura [4]*

[1,2,3,4] Graduate School of Engineering, Tohoku University, Sendai 980-8579, Japan
*E-mail: osamura@eco.civil.tohoku.ac.jp

Abstract

Knowing phytoplankton community compositions which can be predicted best by the size distribution is urgent as it tightly links with ecosystem functions; for instance, the nutrient cycling. Responses of phytoplankton community compositions to eutrophication and global warming effects are well researched while responses to aquaculture are rarely investigated. In this study, mesocosm experiments were conducted *in situ* and suspended organic particles were size-fractionated. Both Fatty Acids and Stable Isotope ratio were analyzed to study the oyster effect on marine phytoplankton community compositions and their ecological funcitons. The results showed that oysters have significant effects on phytoplankton communities such as the diatom, the green algae and the dinoflagellate in in some size-fractionated water samples.

Keywords: Oyster, Phytoplankton community compositions, Mesocosm, Fatty acids, Stable Isotope ratio

1. Introduction

The community composition of phytoplankton is crucial for ecosystem functions such as nutrient cycling. It can be predicted accurately by its size distribution. Responses of phytoplankton community composition in size distribution to the eutrophication and global warming effects were well researched while responses to the aquaculture have been rarely investigated. However, many aquaculture species such as oysters show size-preferences which means they will choose the food resources inside limited sizes (Dupuy 2000). The size-preferences effect might cause shift in the phytoplankton size distribution which may in turn affect their ecological functions (Sandra 2011).

The experiment occurred in Shizugawa bay (Fig. 1) which is an area affected by tsunami because it has more need to focus on the environmental sustainability of oyster farming after the huge damage.

Fig. 1 Study area

2. Methodology

Mesocosm experiments were conducted *in situ* in Shizugawa bay near the suspended oyster farming area. One mesocosm (Fig. 2) system in triplicate was biomanipulated by the oyster species, *Crassostrea gigas*, while another was not treated by oyster as control. After 22h, suspended organic particles in the water sample at all mesocosms were fractionated in size by 2 μ m membrane filter, 20 and 75 μ m sieve respectively, which finally filtered into the GF/F filter. Fatty acids (FAs) and stable isotope ratio (δ 13C and δ 15N) of suspended organic particles were analyzed.

Fig. 2 Image of the mesocosm

3. Results

The POC was mainly consisted of 2~20 μ m and 20~75 μ m particles(Fig. 3). Oysters had no significant effect on size-fractionated POC; however, significant decrease was observed on both the specific FAs concentration(Fig. 4) and their ratios(Fig. 5) of diatom/terrestrial plant, green algae/ terrestrial plant and dinoflagellate /terrestrial plant after size fractionation. Specifically, specific FAs concentration of diatom in in 2~20 μ m and 20~75 μ m, green algae in 20~75 μ m and dinoflagellate in 2~20 μ m were significantly decreased by oysters. The ratios of diatom/terrestrial plant in 2~20 μ m and 20~75 μ m, green algae/ terrestrial plant in 20~75 μ m, dinoflagellate/ terrestrial plant in 2~20 μ m were also significantly decreased by oysters..

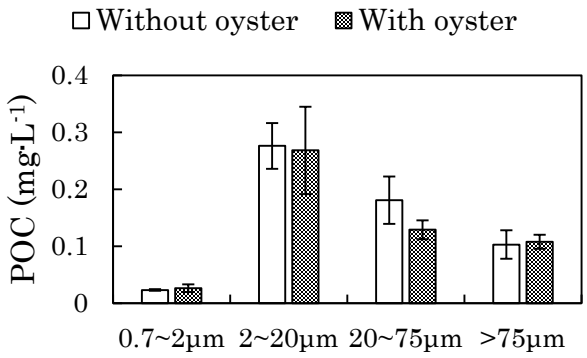

Fig. 3. Comparison between Without oyster (white bar) and With oyster (dark bar) for POC concentrations (expressed as mg·L^{-1}; Mean±SD, n=3) in each size-fractionated water sample.

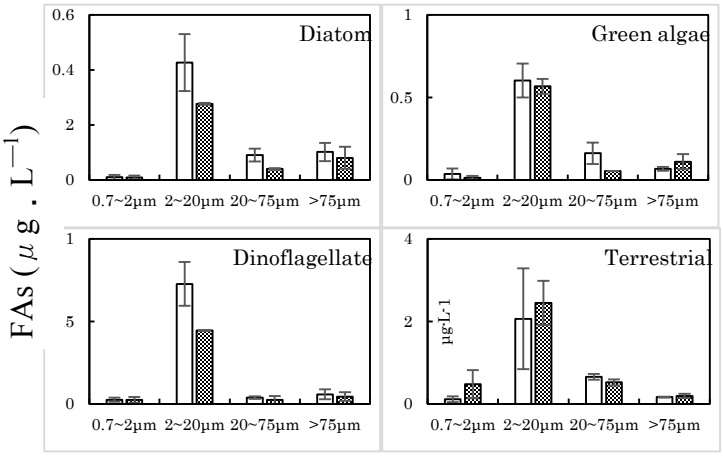

Fig. 4. Comparison between Without oyster (white bar) and With oyster (dark bar) for specific FAs concentrations (expressed as μg·L^{-1}; Mean±SD, n=3) in each size-fractionated water sample.

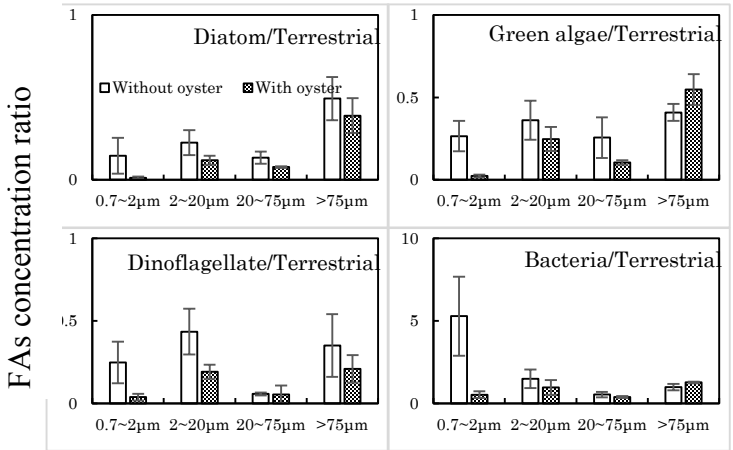

Fig. 5. Comparison between Without oyster (white bar) and With oyster (dark bar) for specific FAs ratio in each size-fractionated water sample.

4. Discussion

Although oysters had no significant effects on size-fractionated POC which represent for the quantity of phytoplankton communities, they showed significant effects on the specific FAs concentration ration which represent for the quality of phytoplankton communities. The results of decrease in each ration indicate that oysters have selective predation on organic matters with different origins. Oysters mainly preyed on diatom in both 2~20 μm and 20~75 μm size while the green algae and the dinoflagellate were mainly preyed in 20~75 μm and 2~20 μm size respectively. This may indicate that oysters showed different size-preferences in different phytoplankton species. In addition, the community composition of phytoplankton in both size distribution and species number might be affected by the predation of oysters.

5. Conclusions

Oysters showed significant effect on phytoplankton communities such as diatom, green algae and dinoflagellate in some size-fractionated water samples. Oysters have selective predation on phytoplankton with different size while 2~75 μm size were mainly preyed on. They also have selective predation on organic matters with different origins while the specific FAs concentration ratios significantly decreased. The farming of oysters probably shifts the size distribution of marine phytoplankton, which may further affect the ecological functions of marine ecosystem.

References

Dupuy, C., Pastoureaud, A., Ryckaert, M., Sauriau, P.G., Montanié, H., (2000). Impact of the oyster *Crassostrea gigas* on the microbial community in Atlantic coastal ponds near La Rochelle. *Aquat. Microb. Ecol.* **22**, 227-242.

Sandra E. Shumway (2011). Shellfish Aquaculture and the Environment,

Evaluation of new sewage treatment system using anaerobic membrane bioreactor

○Toshiki Sugo[1] , Ryoya Watanabe[2] , Yu-You Li[1,3]

[1,2]Graduate School of Environmental Studies, Tohoku University, Sendai 980-8579, Japan
[3]Graduate School of Engineering, Tohoku University, Sendai 980-8579, Japan
*E-mail: yyli@epl1.civil.tohoku.ac.jp

Abstract

Possibility of phosphorus removal was evaluated by adding flocculants ($FeCl_3$) in Submerged Anaerobic Membrane Bioreactor(SAMBR). Two ways of experiments were conducted. One is flocculation test for membrane permeate water to evaluate possibility of post-stage processing. And 80% of phosphorus was removed by adding flocculants of molar ratio 1.5. In another experiment, flocculants were directory added to the reaction tank. As a result, COD removal rate and methane production was increased. Progress of membrane fouling was changed by density. But in spite of having added enough flocculants , T-P removal rate was only up to 25%.

Keywords : anaerobic, membrane, flocculation, SAMBR, sewage

1. Introduction

Recently the sewerage treatment method of the energy-saving and low carbon emission model came to be demanded. In this study, sewage treatment of laboratory scale was carried out by SAMBR which is space - saving and energy - generate system. Then flocculants were added SAMBR system to evaluate phosphorus removal and effect for SAMBR system. At first, flocculation test for the permeate was carried out to evaluate post-stage processing. After that, Consecutive experiments by adding flocculants to reaction tank was carried out to evaluate phosphorus removal, membrane fouling, gas production and water quality.

2. Materials and Methods

2. 1. Experimental facilities

As shown in Fig.1, SAMBR reactor with 6L working volume was used in the experiment. The reactor had a submerged membrane which was made by in the reactor. The materials of the membrane are polyethylene chloride. And the membrane surface area is 0.116㎡. An aperture diameter of the membrane is 0.2 μ m. Pump were used for influent and effluent water. And HRT was controlled by timer. The gas which was generated by reactor was diffused from bottom of reactor to reduce membrane fouling and circulate sludge. And the gas was collected by a gas holder and measured everyday. The temperature in the reaction tank was set on 25 degrees Celsius by the water jacket which I attached outside. Ferric chloride was used for flocculant.

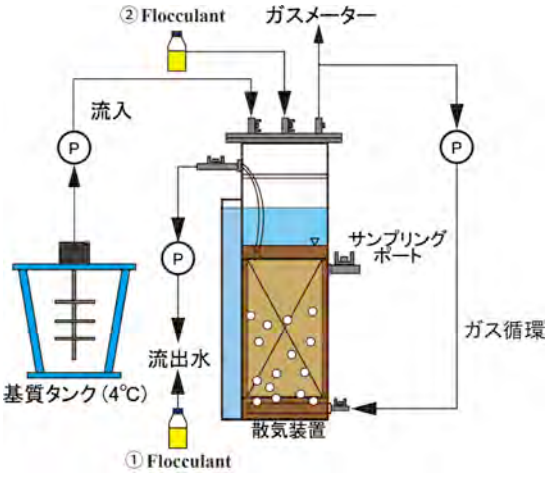

Fig.1 Schematic diagram of SAMBR

2.2. Experimental condition

As shown in table 1, artificial sewage was used in thisexperiment. COD_{Cr} was adjusted to 500mg/L. Before adding flocculant in the reactor, control system was operated with gradually shortening HRT(HRT 24 → 8 h). Then $FeCl_3$ was added to permeate and phosphorus removal rate was measured to evaluate the possibility of post - stage processing. After that, flocculants ware added to the reactor at HRT 8 h. The injection of the flocculant was carried out with a pump.

Table.1 Artificial sewage property

COD	mg/L	499 ± 94
BOD	mg/L	334 ± 78
T−P	mg/L	4.54 ± 0.7
T−N	mg/L	49.2 ± 5.3
pH	-	7.2 ± 0.2

2.3. Analytical method

COD, BOD, T-P and T-N of influent and permeate water were analyzed regularly. In the mixture in the reaction tank, SS and VSS were analyzed. COD was analyzed according to APHA Standard Method. BOD, SS, VSS, T-N and T-P were analyzed according to 下水試験方法（1989）

3. Results and Discussion

3.1. Flocculation test for permeate of SAMBR

Result of flocculation test was shown in Fig. 2. $FeCl_3$ were added by changing molar ratio of iron for phosphate - phosphorus. As shown in Fig. 2, as molar ratio rises, the removal of phosphorus increased. In molar rario 1.5, 80% of phosphorus were removed (4.48→1.0 mg-P/L). From this result, It was found that phosphorus can be removed enough in post-treatment.

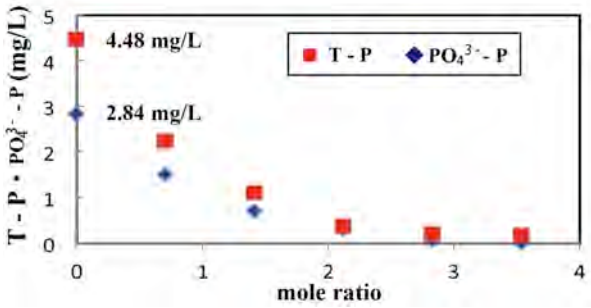

Fig. 2 Flocculation test for permeate of SAMBR

3.2. Direct addition to the SAMBR

(a) Membrane pressure, (b) COD, (c) BOD, (d) T-P, are shown in Fig. 3. Treatment performance is shown in table. 2.

From Fig. (a), it's found that membrane pressure increase speed increased by adding low concentration of $FeCl_3$ (molar ratio 1.0～1.5), but it decreased by adding high concentration of $FeCl_3$ (molar ratio 2.0～2.5).

From Fig. (b) and Table. 2, the COD removal rate rose (97% →98.5%) by adding $FeCl_3$. This is because a particle size in the reactor became big by adding flocculant. Effluent of BOD was always less than 20 mg/L. As a result of having calculated the COD mass balance, COD was converted into methane effectively in comparison with before addition.

From Fig. (d), in spite of having added enough flocculant, only up to 25% of phosphorus were removed. By measuring Fe of effluent, it was found that 75% of Fe were flowed out. From this, most Fe may not react with phosphorus. According to the water quality test method of Ministry of Land, Infrastructure and Transport[1], it says "under the anaerobic condition at the bottom of the lake, a part of formed iron phosphate elutes". Combined with this study, it is found difficult to remove phosphorus by directory adding $FeCl_3$ to the reactor.

4. Conclusion

・At low molar ratio(1.0～1.5), membrane fouling is reduced. But, at high molar ratio(2.0～2.5), that turns worse.

・COD removal rate is increased from 97 % → 98.5 % by adding FeCl. From COD mass balance, It was found that adding FeCl increase methane production.

・In spite of having added enough flocculant, only up to 25% of phosphorus were removed by adding directory to the reactor. ・But, from flocculation test for permeate of SAMBR, phosphorus was removed enough (4.48 → 1.0mg/L) by adding 1.5 molar ratio $FeCl_3$.

< Reference >

1) The water quality test method : Ministry of Land, Infrastructure and Transport

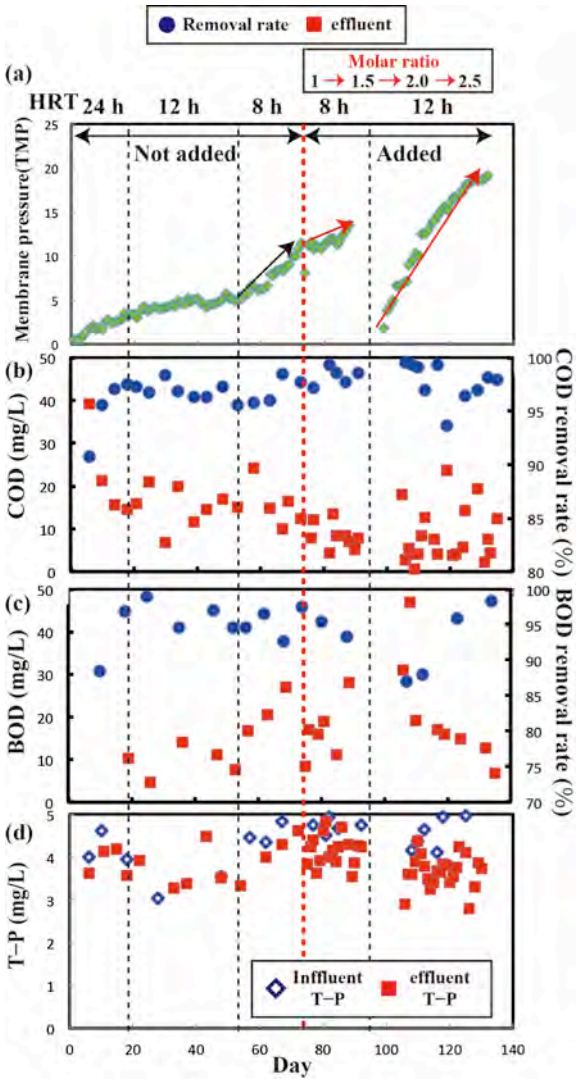

Fig. 3 (a) Membrane pressure (b) COD (c) BOD (d) T-P

Table. 2 Treatment perfprmance

HRT	HRT24	HRT12	HRT8	HRT8 flocculant	HRT12 flocculant
COD effluent (mg/L)	17.1	15.2	15.6	9.1	8.3
COD removal rate (%)	96.8	96.8	97.0	98.3	98.5
BOD effluent (mg/L)	10.2	9.3	18.3	18.2	13.5
BOD removal rate (%)	96.9	96.8	95.3	96.0	96.6

Table.3 Removal rate of phosphorus

Molar ratio	Not added	1.0	1.5	2.0	2.5
Removal ratio of T-P (%)	9.9	10.9	18.7	23.6	25.4

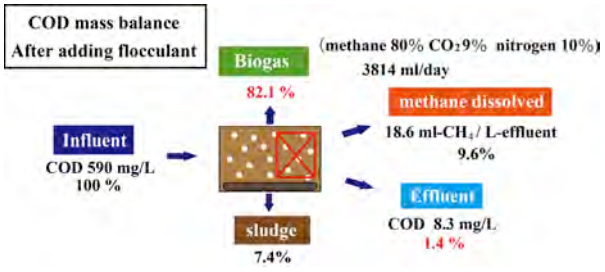

Fig. 3 COD mass balance

Study of the start-up and inhibition process of Anammox reaction in UASB Reactor

○Yanlong ZHANG[1], Shilong HE[2], Haiyuan MA[1], Qigui NIU[1], Yu-You LI[1,3]*

[1]Graduate School of Engineering, Tohoku University, Sendai 980-8579, Japan
[2]School of Environment Science and Spatial Informatics, CUMT, Xuzhou, 221116, China
[3]Graduate School of Environmental Studies, Tohoku University, Sendai 980-8579, Japan
*E-mail: yyli@epl1.civil.tohoku.ac.jp

Abstract

The Anammox system was started up with 2L of activated sludge and 3L of anaerobic digestion sludge in a UASB reactor. After 140 days enrichment, the Anammox system was successfully started up. The ammonium removal efficiency reached to near 99.5%.Substrate concentration shock, nutrient salt shock and nitrogen loading shock were also investigated in the experiment. The results indicated that the Anammox process was very sensitive to the change of operational conditions, and the recovery process took 2~3 months long time. The reaction ratio of consumed nitrite to ammonium (R_S) and produced nitrate to consumed ammonium (R_P) were also studied in long-term experiment and short-term experiment.

Keywords: Anammox, inhibition, recovery, free ammonium (FA), free nitrite acid (FNA), reaction ratio

1. Introduction

As an innovative and sustainable biotechnology for nitrogen removal with the advantage of low-cost and low sludge production , anaerobic ammonium oxidation (Anammox) process has been increasingly valued in the wastewater treatment with low carbon to nitrogen (C/N) ratios. In this process, Planctomycete type bacteria combine ammonium and nitrite to generate nitrogen gas under anaerobic condition without organic carbon source. Eq. (1) describes the nitrogen removal reaction by Anammox process.

$$NH_4^+ + 1.32NO_2^- + 0.066HCO_3^- + 0.13H^+ \rightarrow 1.02N_2 + 0.26NO_3^- + 0.066CH_2O_{0.5}N_{0.15} + 2.03H_2O \quad \cdots\cdots\cdots\cdots (1)$$

The reaction characteristics of Anammox process results in 60% reduction of energy consumption as well as 90% reduction of CO_2 emission that minimize the carbon footprint in wastewater treatment plant. However, challenges in fast start-up and steady operation of Anammox system limited its application and industrialization. The long doubling time (10d~14d) and low cell yield ($0.11 gVSS g^{-1}NH_4^+$-N) of Anammox bacteria results in a quite long startup period of Anammox reactor. Both substrates can exert inhibitory effects on Anammox process, high substrate concentration can easily cause the decrease of Anammox activity and the loss of the stable operation.

The aim of this study focused on the evaluation of the start-up process in UASB reactor. Substrate inhibition and recovery process was also studied in the experiment.

2. Materials and Methods

2.1. Experimental facilities

As shown in Fig.1, UASB reactor with 5L working volume was used in the experiment. The reactor had a height-diameter ratio of 8:1 and made with strong plexiglass. Water jacket was used to control the temperature in the range of 33±1℃. The reactor was covered with light-weight shading fabric to avoid the growth of photosynthetic microorganism which would produce oxygen. Influent pumps were controlled by timer (on 1min, off 1min) to intermittently provide substrate into the reactor. Gas production was measured with homemade Gas-holder.

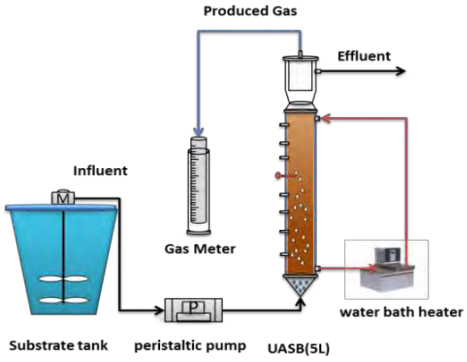

Fig. 1 Experimental setup

2.2 Experimental procedures

3L of nitrification sludge and 2L of anaerobic digestion sludge were inoculated into the reactor. Effluent pH was controlled in the range of 7.6~8.5.The reactor was fed with synthetic wastewater, the initial HRT was set at 24 hours. NLR increased gradually by changing HRT at a constant substrate concentration of 210mg-N/L, and finally reached to 1.68 g/L/d. Then, the influent TN concentration was doubled without change of NLR. After the TN removal efficiency decreased to 40%, the influent TN concentration was returned to the initial level of 210mg-N/L to study the effects of substrate shock. Nutrient salt shock and over loading shock were also investigated. When the Anammox reaction was totally recovered, TN concentration was increased to 1250mg/L to raise the NLR to 10g/L/d.

3. Results and Discussion

3.1. Start-up phase

As shown in Fig.2, N_2 gas production rate and TN removal efficiency began to increase from 100d. Gas component analysis indicated that over 98% of the produced gas was N_2.

The theoretical N_2 gas production was basically consistent with the measurement value that confirmed the Anammox reaction. Accompany with the occurrence of Anammox activity, pH also increased due to the consumption of HCO_3^- which was provided as inorganic carbon source and buffer agent. It took around 40 days to achieve the highest ammonium removal efficiency which around 99% and maintain stable.

Accompany with the change of HRT, gas production maintained stable growth. Anammox bacteria further enriched in the reactor. Fig.3 shows the successfully enriched Anammox granular with an average diameter of 1-2mm.

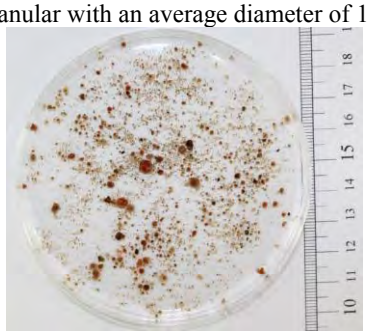

Fig. 3 Enriched Anammox granular sludge

3.2. Inhibition and recovery phase

After doubling the TN concentration at 327d, pH increased to 9.0. Then, 2 times of buffer was added in order to decrease the pH to the optimum range (Fig.2, phase II). Gas production rate and TN removal efficiency rapidly decreased to 420mL/L/d and 40% respectively. As a result, effluent NH_4^+-N and NO_2^--N reached to 100 mg/L and 120 mg/L respectively. The average results obtained from previous studies to evaluate the effects of substrate on Anammox process are presented on the basis of the Free Ammonia (FA) and Free Nitrite Acid (FNA) concentration, due to the fact that FA and FNA are considered to be the true inhibitor compounds. In this study, FA increased to 20 mg/L, FNA decreased during the first 10 days and then increased rapidly to 7μg/L due to the change of pH and NO_2^- concentration (Fig.4, phase II). Similar results were observed in the experiments of nutrient salt shock and overloading shock (Fig.4, phase IV, phase VII). The concentration of FA and FNA were obviously related to the stability of Anammox reactor.

To evaluate the ability of the recovered Anammox system, influent TN concentration was increased to 500mg/L gradually at a constant HRT of 3h, correspondingly, the NLR increased to 4.0g/L/d. The nitrogen removal efficiency decreased with the change of influent TN concentration but soon recovered to previous level, the results that indicated that the nitrogen removal potential of the Anammox system was further improved.

4. Conclusions

(1) Anammox system was successfully started up in 140 days from a mixture of nitrification sludge and anaerobic digestion sludge. TN removal efficiency reached to 90%.
(2) The system was sensitive to the substrate shock, nutrient salt shock and overloading shock. FA, FNA and pH were the factors that affecting the stability of Anammox system.

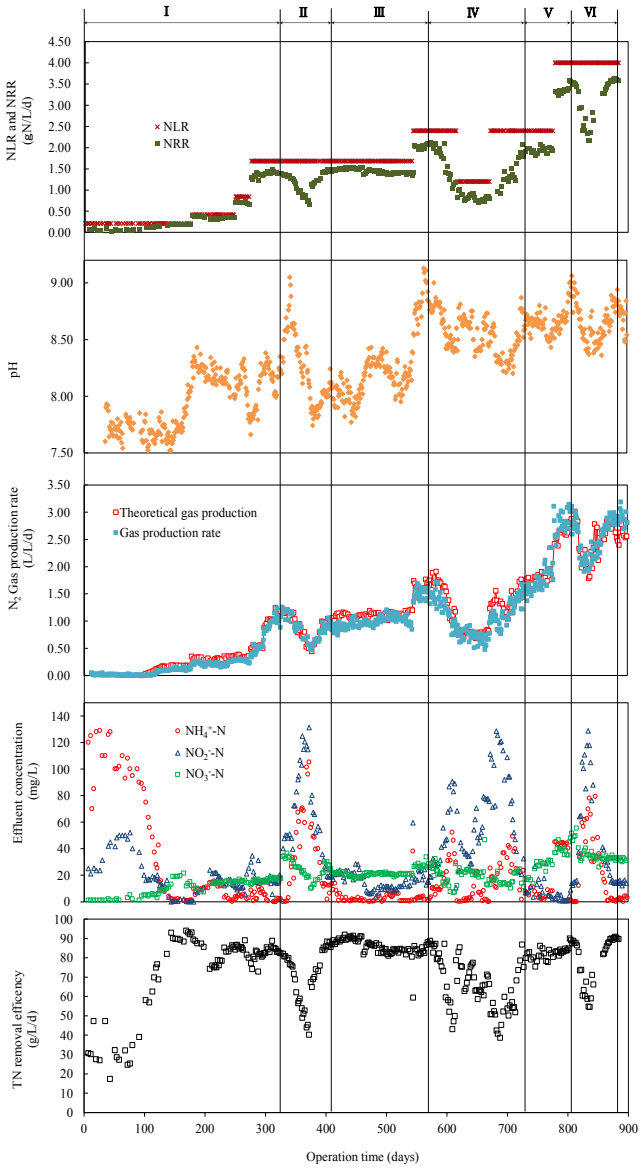

Fig. 2. Time course of Anammox reaction during continuous operation

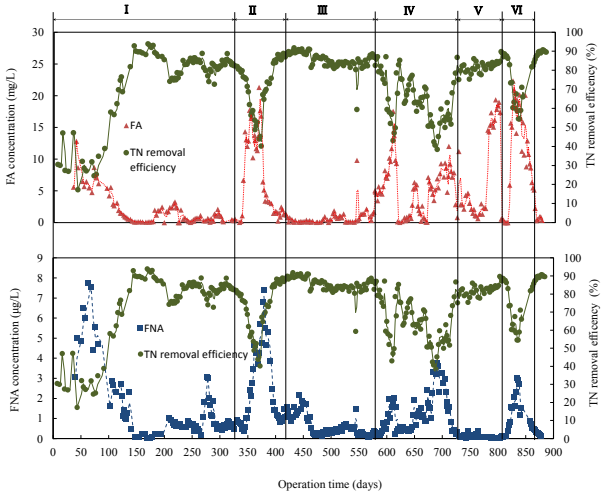

Fig.4. Effects of FA and FNA on reactor performance during different operational stage

Innovation of cool-pavement technology from waste tile

○Nickholas Anting

Universiti Teknologi Malaysia
E-mail: nickholasanting@gmail.com

PRODUCT INFORMATION

Product Summary

The typical paving materials used today are mostly dark in color and solid, which predominantly absorb and retain more solar heat than reflect it. This ordinary type of construction pavement material is one of the major the contributors to the urban heat island (UHI) occurrence. If the solar radiation is directly exposed to the materials, it will cause higher elevation in ground temperature. Large amount of heat that is stored in typical pavement may contribute to the heat storage and will affect the surrounding ambient temperature and can cause a simultaneous heat stroke. Although the measure of heat stroke is nearly rare recorded in the country, a future data prediction seems to happen due to urbanization warnings. In order to reducing the urban heat islands, some modification to the existing pavement should be conducted in order to increase the solar reflectance on the surface of the pavement. These strategies can reduce the amount of heat to be absorbed and decline any heat stored by the ordinary pavement. The solar radiation will be reflected by the special anti-store surface material on the top of the surface pavement layer. After the thermal heat being reflected, the pavement will remain at its ambient temperature, thus allowing more convenience to the surrounding temperature.

This study is focusing on the new material for cool-pavement, which is a resin based asphalt surface coating, with special reflective aggregate from waste material. The materials is originally from wasted tiles mix together with sand to improve its physical properties. Different kind of tiles are mixed together to achieve the higher solar reflectivity, which reduce the surface temperature of the asphalt surface. Preliminary development result shown that the composite surface coating materials able to reduce the surface temperature of asphalt surface about 4.4 °C during peak solar intensity. New improvement of the coating material has found that the developed coating material able to reduce the surface temperature of the pavement about 10 °C during peak solar intensity, with surface reflectance more than 0.50. Based on this data, the developed material has a good potential to be used as cool-pavement material, thus reducing the effect of urban heat island.

Product Features and Pictures

CIP-Tech Coating is a new materials innovation which is originally from wasted tiles. It is the combination of three types of selected tiles in the form of aggregate, which are Full Body Porcelain (FBP White Colour), Monoporosa and Porcelain Glaze. The combination of these tiles aggregate are attached together as surface coating materials by using epoxy.

This product able to increase the surface reflectivity of asphalt surface from 10% - 15% into 50% - 55%, which mean that the surface temperature can be reduce up to 20 °C. CIP-Tech Coating is suitable to be applied at asphalt parking lot and pedestrian walk.

CIP-Tech Coating Model

Application of CIP-Tech Coating at Actual Parking Lot

MATERIALS INGREDIENT AND PROPERTIES

CIP-Tech Coating is made from the combination of two types of wasted tiles, with the specific proportion as mentioned below:

Types of Tiles	Proportion Based on Weight, %	Specific Gravity, kg/m^3	Design Weight for 1m^2 (for 0.002 m - 0.003 m thickness), kg/m^2
FBP White Colour	50	1366.7	1.708
Monoporosa	50	1042.7	1.303
Porcelain Glaze	0	1248.0	0.000

By considering 50% of losses, add 50% to be included in the design. Then,

Types of Tiles	Proportion Based on Weight, %	Addition of 50% for wastage, kg/m^2
FBP White Colour	50	2.562
Monoporosa	50	1.955
Porcelain Glaze	0	0.000
	TOTAL WEIGHT	4.517

MANUFACTURING PROCESS

1. Materials Collection

This activity involve with the selection of the materials from the supplier company that able to meet our materials requirement needs.

Lorry for transportation of the materials is need to transport the materials from the materials supplier to manufacturer.

Raw materials (unused wasted tiles)

2. Crushing the Materials

The materials collected from tiles manufacturer crushed by using crusher into a form of aggregate.

Different types of tiles should crushed separately.

Crusher Machine

Tiles aggregate after crushing

3. Sieving Process

This is perform in order to obtain the size of aggregate between 1.0 mm to 2.0 mm.

Collect the sieved aggregate and put into gunny sack separately.

4. Washing Process

This process is important to remove the dust and impurities.

Use clean water.

Immerse the materials into clean water for 24 hours period.

……..